國立交通大學

加速器光源科技與應用學程

碩 士 論 文

游離輻射對電阻式記憶體的影響之研究

A Study on Effect of Ionizing Radiation on Resistive Random Access Memory

研 究 生：張克勤

指導教授：崔秉鉞 教授

許博淵 博士

中華民國一百零一年十月

游離輻射對電阻式記憶體的影響之研究

A Study on Effect of Ionizing Radiation on Resistive Random Access Memory

研究生:張克勤　　Student: Ko-Chin Chang

指導教授:崔秉鉞　　Advisor: Bing-Yue Tsui

Bor-Yuan Shew

國立交通大學

加速器光源科技與應用學程

碩士論文

A thesis
Submitted to Graduate Program for Science and Technology of Accelerator Light Source
National Chiao Tung University
in Partial Fulfillment of the Requirement
for the Degree of Master
in
2012
Hsinchu, Taiwan, Republic of China

中華民國一百零一年十月

游離輻射對電阻式記憶體的影響之研究

研究生: 張克勤　　指導教授: 崔秉鉞

許博淵

國立交通大學 加速器光源科技與應用學程

摘要

在本論文中,我們對游離輻射對電阻式記憶體 (RRAM)產生的影響進行研究,其中游離輻射包括極紫外光 (EUV)以及 X-ray。

我們所使用的 RRAM 是以 5 nm 的二氧化鉿作為介電層。在 RRAM 的電性方面,討論切換特性、記憶窗口、資料儲存持久性以及耐久度等特性受輻射的影響。在切換特性以及記憶窗口的方面,看不到任何變化,表示經由輻射照射後所產生的電子-電洞對不會影響 RRAM 的操作。另一方面,資料儲存的持久性也不受輻射影響,在照射前後都顯示出良好的儲存持久性。這是因為在室溫下氧空缺擁有較低的遷移率。

此外,我們也觀察已儲存的記憶狀態經過輻射產生的變化。元件在照射前分別被設定在高阻態 (HRS)以及低阻態 (LRS),並且在照射後馬上進行量測。對於照射前被設為低阻態的元件,其本身的電阻值經過照射沒有太大的改變;反之,在照射前被設為高阻態的元件,有部分元件在照射後阻值改變。此外,阻值改變的元件百分比隨著輻射的總劑量增加而增加。這是因為在低阻態時,氧化層中有多數的氧空缺形成電流導通路徑,以至於經由照射產生的缺陷不會影響低阻態的阻值。然而,當元件處於高阻態的狀態下時,在氧化層中只存在零星的氧空缺,

所以比較容易被輻射所產生的缺陷影響，並且此影響機率會正比於照射輻射之總劑量。一部分的高阻態元件經由輻射阻值會變高，表示氧化層被輻射退火，使得氧化層內的缺陷變少，另一部分的元件經由照射後阻值變低，表示輻射產生的缺陷有可能將零星的氧空缺連成一條電流導通路徑。不過，改變阻值的高阻態元件可由正常的操作回覆到一般高阻態。此外，元件的持久性之劣化會隨著輻射的總劑量增加，這是因為在不斷切換阻態時，在氧化層中即會產生缺陷，因此，當照射產生額外的缺陷時，即有可能使氧化層產生崩潰，造成元件回不到高阻態。最後，在同樣的劑量下，X-ray 所造成的傷害比 EUV 來的輕微。

本論文顯示 RRAM 有極好的抗輻射能力，因此，在元件尺寸微縮時，EUV 微影技術將會是一個好的解決方案。

A Study on Effect of Ionizing Radiation on Resistive Random Access Memory

Student: Ko-Chin Chang

Advisor: Bing-Yue Tsui
Bor-Yuan Shew

Graduate Program for Science and Technology of Accelerator Light Source
National Chiao Tung University

Abstract

In this thesis, the effect of ionizing radiation, including extreme ultra-violete (EUV) irradiation and X-ray irradiation, on the characteristics of Hf-based resistive RAM (RRAM) is investigated.

RRAM device with 5-nm-thick HfO_2 is used. The effect of radiation on the switching characteristics, memory window, retention, and endurance performance of RRAM is studied. The stable of the switching characteristics and the memory window implies that defects generated by irradiation don't affect the operation of RRAM. On the other hand, the retention performance exhibits good radiation hardness since the oxygen vacancies have low mobility in the dielectric layer at room temperature even after the irradiation.

The change of the memory state is measured as well. The RRAM devices are set to the low resistance state (LRS) and high resistance state (HRS) before irradiation, and the memory state is measured right after irradiation. The devices in the LRS initially don't exhibit resistance change after irradiation, while some devices in the HRS initially change their resistance after the irradiation. Besides, the percentage of failed devices increases with the increase of the total irradiation dose. This is because

that there are several filaments in the oxide layer in the LRS so that the irradiation generated defects would not affect the resistance. However, when the devices are in the HRS, sporadic oxygen vacancies in the oxide layer might be affected by radiation when the total dose increases. The increase of resistance after irradiation implies the oxide layer is annealed by irradiation, reducing defects in the oxide; while the change to the lower resistance means the defects might bridge the oxygen vacancies in the oxide layer. The changed HRS states can be rewrite through a regular switching process. Moreover, the endurance performance of RRAM degrades after the X-ray irradiation, and the number of the devices having degradation in the endurance performance increases with the total irradiaiton dose. This result suggests that through lots of switching cycles, defects generated by irradiation might still enhance the possibility for oxide breakdown. Finally, the effect from EUV is stronger than that from X-ray at the same total dose. The difference between EUV and X-ray irradiation damage effect on RRAM is because the calculation method of the total dose leads to the total flux of X-ray being much less than that of EUV.

This work exhibits that RRAM has good immunity against radiation Hence, EUV lithography could be a good solution for the RRAM when the device is scaling down.

誌謝

此篇論文能順利的完成，承蒙許多人的幫助及鼓勵，使我可以去克服各種困難，同時也成長很多。謹以此文來表達我無限的感謝。

首先，感謝我的指導教授 崔秉鉞老師。在培養學生研究的能力上盡心盡力，從實驗的規劃到進行，甚至碰到瓶頸都耐心的指導我並詳加討論，讓我成長成一個有能力獨立構思實驗的人。更重要的是老師剛正嚴謹的研究態度，對於任何事情要追根究底，不能得過且過，這對於我日後的思考有莫大的幫助，受用一生。

再來是感謝國家同步輻射中心及交通大學奈米中心和國家奈米實驗室提供優良的實驗環境及設備，以及幫助過我的工程師與技術員們，使我實驗能順利完成。

最後要感謝實驗室的同學以及學長們在實驗上的幫助，不管是機台的訓練、實驗問題的協助或是珍貴的實驗經驗與知識都熱心與我分享。

再次由衷的感謝以上諸位的幫忙，此論文才得以完成。在此將這篇論文獻給對我付出的你們。

Contents

Table Captions

Chapter 1

Chapter 3

Figure Captions

Chapter 1

Chapter 2

Chapter 3

Chapter 1
Introduction

1-1 Extreme Ultraviolet Lithography Technology

According to Moore's law, the number of transistors on an integrated circuit chip continuously increases. Therefore, the scaling down of device geometry and patterning resolution becomes an important issue. The current mainstream lithography process is using 193 nm argon-fluoride excimer laser as the light source in conjunction with the immersion lithography technology. However, the next generation technology node demands for 15 nm half-pitch, which is almost ninth of 193 nm, makes the current lithography technology face a large challenge. To overcome the physical limitation of lithography, the light source with shorter wavelength should be use. Hence, extreme ultraviolet lithography (EUVL) attracts more and more attention in recent years [1-3].

Electron-beam (E-beam) writing is another potential patterning technology with resolution beyond 22 nm. Instead of using photo mask, E-beam writing technology writes patterns directly by narrow electron beams, leading to high resolution. Besides, without using photo mask, E-beam writing is almost free from the troubles caused in the traditional optical lithography technology, and has high feasibility for pattern design. However, it has a fatal defect. Long writing time leads to low throughput, which leads E-beam writing just be suitable for production of multiple but low volume of logic ICs. Compared with E-beam writing, EUVL uses optical systems, which means that it has many similarities with conventional lithography process. Therefore, some mature technology, like using the binary masks, could support resolution of EUVL down to nodes under 15 nm [4-6].

The most different part of EUVL relative to the current lithography technology is the light source, the extreme short wavelength of 13.5 nm. This short wavelength brings several problems for application because the light will be absorbed by all materials. For this reason, two different parts with conventional lithography systems occur [7-8]. First, instead of conventional refractive optical system, the optical systems for EUVL should be designed as reflective system. However, the reflectivity of EUV at near-normal incidence is too low for singular material. To increase the reflectivity, multi-layer structure composed of molybdenum and silicon were used. By this multi-layer, the reflectivity of EUV can be improved to 70%. Nevertheless, the quality of the multi-layer becomes a critical point. Few defects might increase the surface roughness of the multi-layer, leading to pattern distortion. The second difference is that the EUVL needs a highly vacuum environment to avoid the absorption by airs. Demand of highly vacuum environment directly increases the cost of EUVL.

Recently, TSMC and Intel are both taking advantage of a recent decision by ASML to sell off up to 25 % of its equity and create a 'customer co-investment program' to share the costs and risks of developing both EUV lithography and lithography systems that can handle 450 mm wafers [9]. Therefore, even there has some issues to be solved, EUVL is still the most attractive technology for next generation.

1-2 Radiation Damage Issues

Most of the researches on radiation damages on semiconductor devices are based on the radiation-rich environment. An ionizing radiation environment has various high energetic photons or particles, such as X-ray, gamma ray, electrons, protons, and alpha particles. These photons or particles might lead to some degradation in performance

of devices, even cut down the lifetime of devices. However, except the application environment, the fabrication process of semiconductor devices might also face the radiation damage issues. Reactive ion etching (RIE) in dry etching process, E-beam writing, and other plasma processes are the possible radiation sources. Compared with the radiation damages in the application environment, the central of a device, such as oxide layer of MOS devices is already capped with metal layers and passivation layers, during the fabrication process those central layers would be irradiated directly. Worst of all, with the trend of devices scaling down, dry etching and high resolution lithography technology is required. Hence, radiation damage under the fabrication process of semiconductors must be considered. EUVL, as a promising technology for next generation lithography, uses the light source with 13.5 nm wavelength. The short wavelength which is in the range of X-ray could also make damages to devices. Hence, this effect should be taken seriously for EUVL.

The basic concept of ionizing radiation is that radiation source that has sufficient energy to break atomic bonds and generate electron-hole pairs. For most of the MOS devices, the most sensitive layer is the gate oxide layer. Fig. 1-1 shows the band diagram of the MOS structure with positive bias applied at gate. As the gate dielectric receives radiation that has energy over its bandgap, electron-hole pairs are generated in the oxide. In the pico second, most electrons will be swept to gate by the positive bias. Part of electrons might recombine with holes. The holes that not be recombined, due to its relatively low mobility compared with electrons, will stay in oxide. Thus, holes play more important role than electrons in the radiation damage issues. Holes trapped in the oxide will lead to a negative flatband voltage shift. After a while, a part of holes might transport to the silicon/silicon oxide interface through trap-hopping process. As holes arrive at the interface, some of them will be trapped in the deep-level trapping site, cause permanent threshold voltage shift. Radiation will also

damage the silicon/silicon oxide interface, building interface traps. As holes hop to the interface, they may capture electrons and create interface traps within silicon bandgap. Interface traps could be charged as positive, negative, or neutral depending on the traps and the silicon surface potential [10].

MOS devices will fail due to threshold voltage shift, subthreshold swing degradation, gate leakage current increase, gain decrease, or even breakdown under radiation environment [11-13]. On the other hand, for memory devices, those problems could be worse. The mainstream of memory devices is flash, which is operated by storing electrons. Hence, the charged state would strongly affected by radiation. Degradation of memory window, program/erase speed, retention, and endurance are the issues for memory devices [14-16].

The radiation damage of SONOS and nano-crystal memory has been studied. Memory window changing and retention and endurance performance degradation are observed in SONOS memory, owing to the traps generation in the oxide nitride layer and defects generation in the tunneling and blocking oxide. On the other hand, the nano-crystal memory has also no performance degradation since the charges are stored in the isolated metallic nano-crystals. Thus, the damage on the oxide layers would not affect the performance [17].

1-3 Background of RRAM

In the present day, memory devices are around our life by embedded in communication tool, like mobile phone, and entertainment tools, like iPod or PSP. The mainstream of these memory devices is flash memory, for its high capacity and MOSFET-like structure. However, the physical limits mentioned before makes a very high barrier for flash device. The leakage current issue is one of the problems for the

scaling down floating gate devices because of its thinner tunneling oxide. The charged floating gate might lose its state. Thus, this issue directly hit the critical point of production line, reliability of devices. Besides, the operating speed is no longer satisfied resent demand, even for floating gate or SONOS. Furthermore, the total number of stored charge would be reduced when the area of the charge trapping region scales down. This implies the shrink of the memory window and the difficulty of the bits controlling [18-19]. To solve these issues, several nonvolatile memory (NVM) technologies like phase-change memory (PCM), magneto-resistive memory (MRAM), ferroelectric memory (FeRAM), and resistive-switching memory (RRAM) have been proposed to be the potential NVM for next generation. Among the above mentioned devices, RRAM could be embedded in the CMOS fabrication process and already had some achievement. Besides, RRAM has the lower operation power than PCRAM, the lower temperature in the fabrication process than FeRRAM, and the lower fabrication cost than MRAM [20–22]. Table 1 compares the performance of various types of semiconductor memories [23]. Hence, among the above mentioned devices, RRAM is a very promising memory device which is able to defeat the flash memory.

The idea of using the resistance switchable material as NVM has been appeared before 1970s. However, with the rise of flash memory, research on RRAM was not taken so serious, leading to the result that there was no significant breakthrough until recent 10 years. The mainstream material for the dielectric of RRAM is based on binary oxide, for the feasibility of compacting with CMOS fabrication process. The widely attracted materials include NiO, TiOx, AlOx, ZrOx, and HfOx [24-28].

The operation of the binary oxide based RRAM, which is the structure stacked with metal/insulator/metal (MIM), is applied a strong electric field across top and bottom electrode. Before the regular operation process, at first, an electric field being

able to breakdown oxide should be applied, to build a conduction path for electrons. This step is called the forming process for RRAM, and the formed conduction path is called conducting filament [22]. The conducting filament is constructed by defects, which in the binary oxide are the oxygen vacancies. As shown in Fig.1-2, after the forming process, the oxide film is full of conducting filaments, leading to a low resistance state (LRS) for oxide. Going through the forming process, RRAM sample can be operated at relatively low voltage compared with the forming voltage. For the different oxides, the operating voltage has different polarity to switch the resistance. One is applying the same polarity of voltage, and the oxide can switch between LRS and HRS (high resistance state), which is the so-called the unipolar device [29]. Another one is applying opposite polarity of voltage for switching, which is called the bipolar device [24]. The main different between the two devices is the process of switching from LRS to HRS, which is the so-called reset process. Reset process is the break of conducting filament, caused by Joule heat for unipolar device and recombination of oxygen vacancies for bipolar device. After reset process, apply an appropriate voltage to reconstruct the conducting filaments, switching RRAM from HRS to LRS.

1-4 Motivation

As mentioned, EUVL is one of the potential technologies for next generation lithography. Nevertheless, the wavelength of 13.5 nm equals to the energy of 91.85 eV, which is much higher than the bandgap of all dielectric materials and chemical bonding energy. Not only logic ICs but memory ICs will be affected. The radiation damage issue of EUV on MOS capacitors with different dielectric materials, including SiO_2, MOCVD Al_2O_3, HfAlO, HfSiO and ALD Al_2O_3, has been performed by

Po-Hsueh Li [30]. On the other hand, the flash memory devices, including SONOS, and nano-crystal type have also been studied by Chih-Chan Yen [17].

In this work, the radiation damage issue of EUV irradiation on the Hf-based RRAM will be studied. The structure of RRAM contains dielectric layer, just like MOS devices and MIM capacitors. Thus, the operation characteristic might be affected. There are few studies of radiation damage on RRAM [31-32]. The studied on radiation hardness of Cu-doped Hafnium oxide-based RRAM has been published by Yan Wang et. al. in 2010 [31]. The radiation source was ^{60}Co gamma ray to a total dose of 3.6×10^5 rad (Si). The switching characteristics, memory window, stability of memory state storage, retention, and endurance performance have no degradation after radiation exposure. The other study is on the TaO_x-based RRAM, which is published by Lijie Zhang et.al in 2011 [32]. The radiation source is also the ^{60}Co gamma ray. The switching characteristics and the change of the stored memory state are studied in that research. The switching characteristic does not change after irradiation, while several cells in the HRS changes their state after irradiation. The different results between these two works are owing to the different oxide material, leading to the different conduction mechanism. The RRAM with Cu-doped Hafnium oxide is conducting with the metallic ion, while the RRAM with TaO_x is conducting with the oxygen vacancies. In recent years, hafnium oxide has been widely studied as the dielectric layers for the binary-oxide based RRAM. The RRAM with 5 nm HfO_2 has been published by H.Y. Lee in 2008. The memory window is over a hundred times ratio between HRS and LRS, and the endurance performance is up to a million switching cycles [33]. Besides, the forming free HfO_2 has been published by Y.S. Chen et.al in 2009. The cell size of 0.1 μm^2 with 3 nm HfO_2 implies the good scalability of Hf-based RRAM [34]. Based on the above mentioned researches, the studies of radiation damage on the Hf-based RRAM due to EUV source will be

conducted in this work. Also, the 10 keV X-ray was chosen to study the effect of energy of the radiation source.

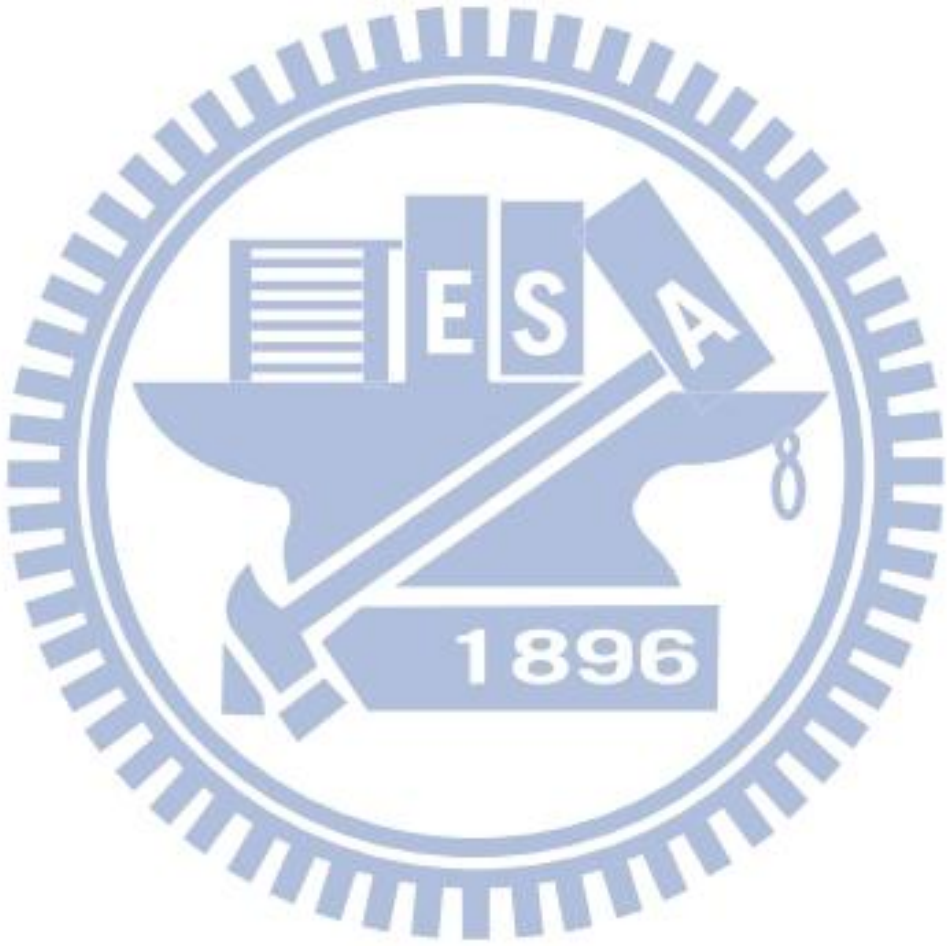

Table 1-1: Comparison of RRAM with other types of memories.

	SRAM	DRAM	NAND Flash	PCRAM	RRAM	MRAM
Cell size(F^2)	> 100	6 -8	4 -5	8 -16	> 5	37
Read Latency	< 10 ns	10 -60 ns	25 μ s	48 ns	< 10 ns	< 10 ns
Write Latency	< 10 ns	10 -60 ns	200μ s	40-150 ns	~ 10 ns	12.5 ns
Energy per bit access	> 1 pJ	2 pJ	10 nJ	100 pJ	2 pJ	0.02 pJ
Static Power	Yes	Yes	Yes	No	No	No
Endurance	> 10^{15}	> 10^{15}	10^4	10^8	10^5	> 10^{15}
Nonvolatility	No	No	Yes	Yes	Yes	Yes

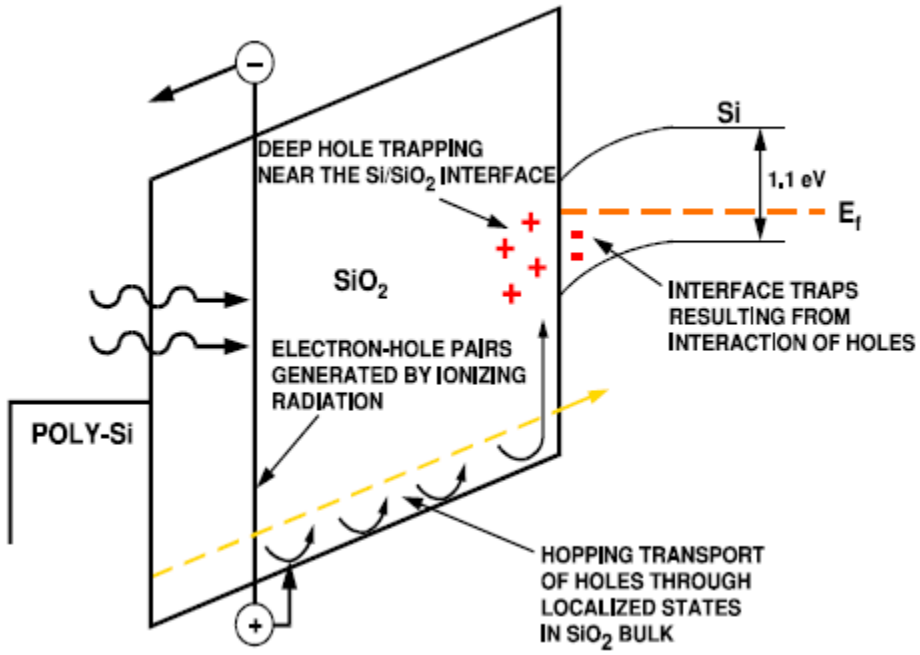

Fig. 1-1: Schematic energy band diagram of ionizing radiation induced electron/hole pairs in the MOS device with a positive gate bias.

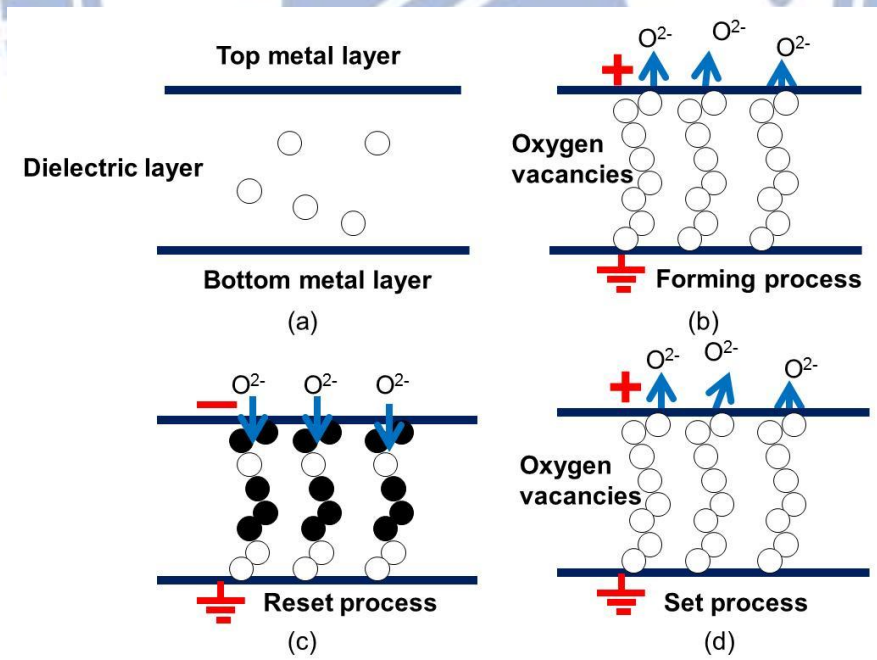

Fig. 1-2: (a) Initial state (b) After forming process (c) After Reset process (d) After Set process.

Chapter2
Experimental Procedure

2-1 Instruments setup

Series of experiments of EUV radiation damage on RRAM devices were implemented at the National Synchrotron Radiation Research Center (NSRRC). The EUV radiation source is produced by the electrons acceleration. The electrons are from an electron gun and are accelerated with a linear particle accelerator (LINAC) into a boosting ring. After several cycles, electrons are accelerated to the specific energy and then are sent into the storage ring through a transport line. Electrons keep a circular orbit in the storage ring; thus, the tangent of its orbit will produce radiation for its different velocity. The beam lines used for experiments are built at the tangent position of storage ring. All the environments for electrons travel are in a ultra-high-vacuum environment. The beamline BL08A is used as the EUV light source and the beamline BL07A is used as the X-ray source. The former has an energy range from 15 to 200 eV and the later has an energy range from 7 to 23 keV.

Different end stations are used in BL07A and BL08A, because the difference of energy ranges. At first, in BL07A, the monochromntor is used to adjust the energy of radiation. The energy is calculated from the formula $2d\sin\theta = \frac{hc}{E}$, where $\frac{hc}{E}$ is the wavelength of radiation, and θ is the Bragg angle. Thus, the energy might not be a specific value since the Bragg angle can't be accurately controlled; for example, 11.402 degree for 10 keV X-ray in this case. Second, in BL07A, which has over 7 keV light source, the photons are almost not scattered by air. Thus, instead of the familiar vacuum chamber, the end station used in BL07A is a big room that can isolate X-ray radiation. Fig. 2-1 shows the instrument setup in BL07A. There is an

ion-chamber with a current meter to calculate the total flux by measuring the current. The current is extracted from the ionizing of gas in the ion chamber, usually with nitrogen. Behind the ion-chamber is a mechanical controllable attenuation plate, with different pieces of Molybdenum plates, to produce different intensities of X-ray. The sample stage used to attach RRAM chips on is right behind the attenuation plate. The above mentioned three stages can be moved, thus we put them near each other as possible as we can, to reduce the effect of air scattering. In order to make sure the X-ray radiation can hit the devices accurately, we first attach an UV sensitive paper on the sample stage and let the light irradiated on the paper. The color at the position irradiated by UV light will change. The more intense the UV light is, the more obvious the change of color. Therefore, we can determine the radiation spot position and estimate the area of radiation spot, which is approximately 0.02 cm^2. We draw an orthogonal coordinates with the spot as the origin. We also marks the vertical and horizontal positions of the device set to be irradiated at the chip edges. Then, we attach the RRAM chip on the paper and adjust the chip position so that the marks coincide with the orthogonal coordinates to make sure that the radiation spot can incident on the device set accurately. The sample stage can be controlled by computer program to move to the position we want. On each RRAM chip, there are total nine device sets were irradiated at the same run.

In BL08A, a vacuum chamber is used as the end station. The end station consists of a sample loaded plate, a dry mechanical pump, two turbo pumps, and an ion gauge. Fig. 2-2 shows the photograph of the above mentioned chamber. The main chamber has several view ports, let us be able to check the position of RRAM chip from different angles. The sample loaded plate in Fig. 2-3 is plug in the main chamber from the top side. To prevent RRAM chips which are not our target from been irradiated during the irradiation, a block plate with windows is used. We put the target RRAM

chip aligned with the window so that the other chips behind the block plate will not be irradiated. For the alignment issue, we used the benefit of visible zero-order light, which contains all energy range of lights in this beam line. Because the zero-order light has much higher energy than EUV, it is impossible to align with the chip directly. Therefore, we let the zero-order light irradiated far from the chip, and align its spot with the crossbar sign in a telescope. Then we fixed the position of telescope, and the crossbar sign is definitely the position of radiation spot. Compared with the higher energy light in BL07A, light in BL08A are more sensitive to air scattering. Therefore, all of the work environments need high vacuum. Our two turbo pumps can make the pressure approximate to the order of 10^{-8} torr, which is our experimental environment.

2-2 Device Fabrication

In this study, hafnium oxide based RRAM is used to investigate the radiation damage effects of EUV and X-ray. The RRAM cells used for EUV irradiation is fabricated at the Nano Facility Center, NCTU. On the other hand, the RRAM cells used for X-ray irradiation experiment are provided by Industrial Technology Research Center.

Fig. 2-4 shows the main process flow of the RRAM used for EUV irradiation. The devices were fabricated on 4” silicon wafer. Before the button electrode fabrication, a 100-nm-thick SiO_2 was deposited by a plasma enhanced chemical vapor deposition (PECVD) system, right after the RCA clean. Because this oxide layer is just used to isolate the button electrode of RRAM with the silicon substrate, its quality is not very important. Thus, PECVD instead of thermal oxidation was selected for its relative short process time. The button electrode consists of

10-nm-thick Titanium and 30-nm-thick Platinum. The double metal layers are in-situ deposited with sputter method. A 300-nm-thick silicon dioxide was then deposited by PECVD as the field oxide. The deposition condition of the PECVD SiO_2 is at 300 ℃, using Silane and N_2O as precursors. Next, active region was opened by Buffer oxide etcher (BOE), through the first patterning process. Hafnium oxide of 5-nm-thick was then deposited by an atomic layer deposition (ALD) system. The deposition condition was at 250 ℃and using TEMAH and water as precursors. The top electrode was deposited in the same condition as the button electrode – Ti (30 nm)/ Pt (30 nm). The titanium layer was used to rubber oxygen ions in the hafnium oxide layer, forming HfO_x/TiO_x layers and improving the migration of oxygen ions. A 300-nm-thick PECVD SiO_2 was deposited as hard mask. The second patterning was performed to define the top electrode pad. A series of wet etching process was applied. First, BOE was used to etch the SiO_2 hard mask. Aqua regia, which was mixed with hydrochloric acid and nitric acid at the volume ratio of 3:1, was used to etch Platinum. At the mean time, large area of the photo resist on the remained hard mask would also be lifted. This was the reason why the SiO_2 hard mask is needed. Sulfuric acid was used to ensure the photo resist and the titanium layer were etched completely. Finally, BOE was used to etch the hafnium oxide beyond the top electrode to expose the bottom electrode. The TEM image of the RRAM is shown in Fig. 2-5.

The structure of RRAM devices provided by ITRI is briefly described here. The detail process flow and device performance have been published in literature [33]. The main device part has a structure of titanium nitride (50 nm), hafnium oxide (5 nm), titanium (10 nm), and titanium nitride (50 nm). The top electrode connects with a aluminum copper metal line. A 200-nm-thick silicon dioxide is used as the passivation layer, leading to the result that EUV will be almost absorbed. The TEM image is shown in Fig. 2-6.

2-3 Electrical Characterization Techniques

The measurement conditions are described in this section. All measurements used the semiconductor parameter analyzer of modal Agilent 4156C. Resistive switching characteristics and retention characteristics were measured on both the EUV and X-ray irradiated devices. Endurance characteristics were measured only on the X-ray irradiated devices because the RRAMs used for EUV irradiation, fabricated at NFC, do not have good enough endurance characteristics. The resistance values of high resistance state and low resistance state are determined as the voltage divided by current at +0.1 V and -0.1 V, respectively.

In order to compare the characteristics before and after irradiation, it is much more convincible if we can use the same devices. Thus, the memory characteristics must be measured and recorded in advance. The definitions of memory characteristics and methods of measurements before and after irradiation are described as follows.

(A) Restive switching characteristics and memory window

For the RRAM with a simple MIM structure in this study, the bottom electrode is always grounded. The bias determining set or reset process is applied on the top electrode. For the devices used in EUV experiment, the voltage sweeping range is from 0 to 2 V for the set process and from 0 to -2 V for the reset process. On the other hand, the sweeping range of the devices used in X-ray experiment is from 0 to 1.5 V for the set process and from 0 to -1.4 V for the reset process. The reason for choosing different measurement condition is to produce more obvious memory window on the devices used in EUV experiment. Current compliance was set to 1 mA. The current compliance is a big issue for the simple 1R structure, especially for the reliability. If the current compliance is set below 1 mA, current overshooting will happen in the set

process because of the parasitic impedance of the measurement instruments [35-36]. Hence, the current compliance was set to 1 mA for all measurements.

To compare the devices before and after irradiation, four to six devices were measured in advance. Each irradiated device was conducted ten switching cycles, which means the device went through ten times set and reset processes. After irradiation, same device was measured in the same measurement condition for ten cycles again. The I-V curves and memory windows in these set/reset cycles were recorded.

(B) Retention

Retention is a significant reliability specification for non-volatile memories. It is defined as the variation in the high resistance state and low resistance state as a function of storage time at specified storage temperature. In this study, seven to twelve RRAM devices were tested for retention performance. The resistance was measured by applying +0.1 V on the top electrode and sampling the current for two seconds. Before irradiation, devices were set to high resistive state and low resistive state respectively. Then the resistance of each device was measured at every specific time after the initial resistance be measured. The total storage time before irradiation is 10^6 sec, at room temperature. After irradiation, the same measurement condition was used on the same device.

(C) Endurance

Endurance is to evaluate if a memory cell after numbers of switching cycles could still have sufficient memory window and retention performance. The typical standard is 10^5 switching cycles for RRAM. However, in this study, the purpose of endurance measurement is not about the tolerance of device itself, but the difference before and after irradiation. Thus, 2000 switching cycles were applied. In addition, endurance test could cause permanent damage to the device so that different devices

were used before and after irradiation. For the pre-irradiation condition and the irradiation conditions to different total doses, eight devices were measured.

2-4 Total dose Calculation

Radiation dosage is important for the study of radiation damage. It is defined as the absorbed dose in matter resulting from the irradiation to ionizing radiation. The unit of dose is ‘”rad”, which is equal to 100 ergs/g. The beam lines at NSRRC are linear light source [37], thus the calculation of the dose absorption rate should based on the linear source model.

In the linear light source model, we first define the particle flux,

$$\emptyset_0 = \frac{N(E)}{A}\ (\frac{counts}{s\ cm^2}), \tag{2-1}$$

where the N (E) is the number of photons that emitted per unit time by the source as a function of energy E, A is the area of the light source. The flux of radiation $\emptyset_0$ decays as a function of distance, so the attenuation of the flux $\Phi\ (x)$ is defined as the following equation:

$$\emptyset\ (x) = \emptyset_0 exp\ \ (-\mu x), \tag{2-2}$$

where μ is the linear attenuation coefficient and it follows the relation

$$\mu = \mu_m \rho, \tag{2-3}$$

where μ_m is the mass attenuation coefficient and ρ is the material density. With the above three equations, the dose absorption rate D_R can be defined as follows:

$$\begin{aligned} D_R &= \frac{E \times \emptyset_0 [1 - exp(-\mu d_{ox})]}{d_{ox}} \times \frac{1}{\rho} \\ &\approx E \times \emptyset_0 \times \mu_m\ (\frac{eV}{sg}),\ for\ \ d_{ox} \ll \mu^{-1} \end{aligned} \tag{2-4}$$

Because of the thickness of gate dielectric layer d_{ox} is much less than the attenuation length μ^{-1}, by Taylor expansion, the approximation can lead to equation (2-4). In

addition, since 1 rad = $6.24 \times 10^{13} \frac{eV}{g}$, the equation (2-4) can be substituted into

$$D_R = \frac{E \times \emptyset_0 \times \mu_m}{6.24 \times 10^{13}} \left(\frac{rad}{s}\right) \quad (2\text{-}5)$$

Equation (2-5) was used to determine the total dose. The factor μ_m depends on material, thus the particular material should be referenced in parentheses all the time such as rads (SiO_2) and rads (Si). In this thesis, the unit rads (SiO_2) is commonly used.

In this work, radiations with two different energies are used. Although the RRAM devices used in each experiment have the same dielectric layer, which is 5 nm hafnium oxide, the different levels of response to irradiation in each experiment are expected. The reason is that material has different absorption probability for radiations with different wavelength, leading to different attenuation length λ. According to the formula of penetration probability $P(x) = e^{-\frac{x}{\lambda}}$, different attenuation length λ will make the penetration probability different, and the absorption probability will be different. Hence, devices irradiated by EUV and 10keV X-ray are supposed to have different results. The detail results and calculation will be discussed in section 3-5.

Fig. 2-1: The instruments used in BL07A. The I_0 in the photo is the ion chamber used to estimate photon flux. The sample stage is where we put the devices on.

Fig. 2-2: End station in BL08A, including main chamber, two turbo pump and a mechanical pump.

Fig. 2-3 The sample loaded plate

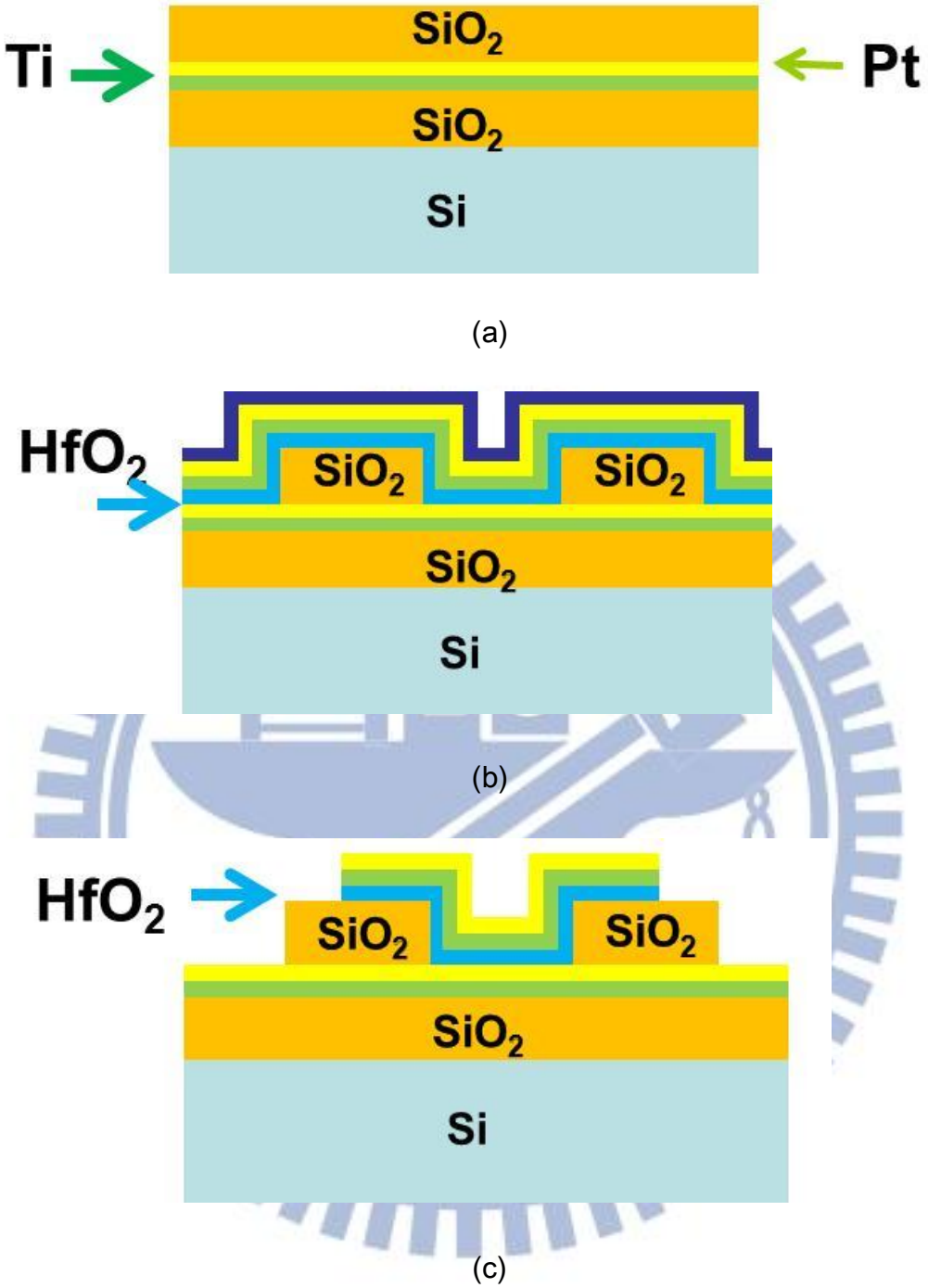

Fig. 2-4: Process flow and cross-sections of RRAM.

(a) Bottom electrode and field oxide deposited on silicon substrate with silicon dioxide, (b) Dielectric layer and top electrode deposition after first patterning, (c) Second patterning to define metal pad and bottom electrode region.

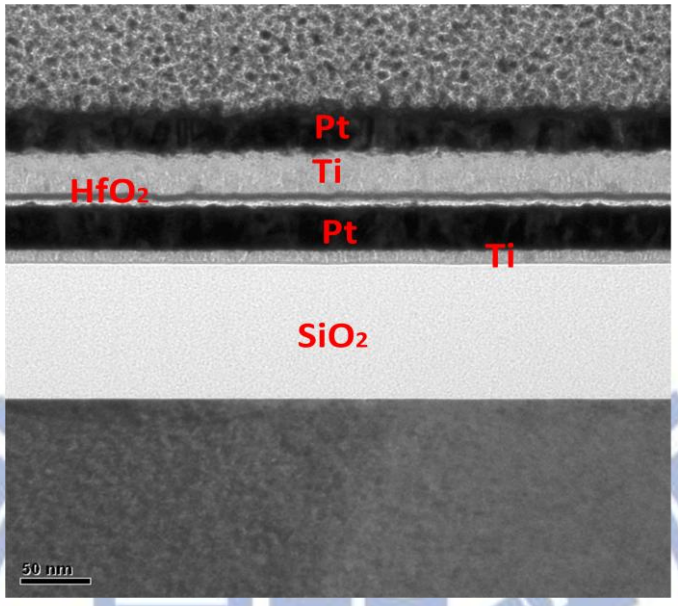

Fig. 2-5: The TEM image of RRAM made in NFC with Hafnium oxide 5 nm

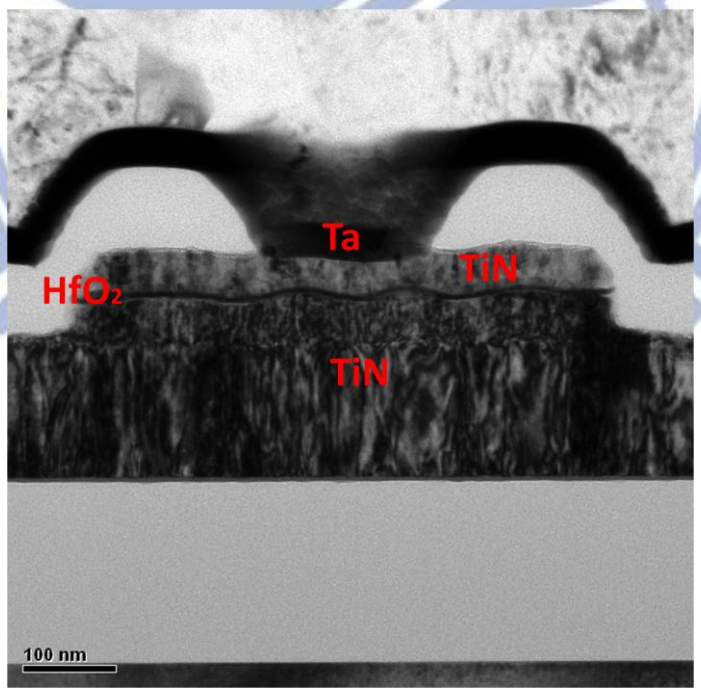

Fig. 2-6: The TEM image of RRAM made by ITRI with Hafnium oxide 5 nm

Chapter3
Results and Discussion

3-1 Introduction

In this chapter, the memory characteristics of RRAM devices before and after irradiation will be discussed. Basic memory characteristics including memory window, retention, and endurance of the memory devices are measured. Also, the different effects between EUV and 10 keV X-ray will be compared. The device dimensions for different total doses of radiation are the same for the sake of easy comparison.

The area of RRAM devices used in the EUV experiment is 628 μm^2, and the area of device used in the X-ray experiment is 0.23 μm^2. The total dosages used in the EUV experiments are 1 Mrads (SiO_2), 50 Mrads (SiO_2), 100 Mrads (SiO_2), 300 Mrads (SiO_2), 600 Mrads (SiO_2), and 900 Mrads (SiO_2). Since there is no difference between the results of RRAM exposed by X-ray to the total dose of 1 Mrads (SiO_2) and 100 Mrads (SiO_2), the experiment with 50 Mrads (SiO_2) X-ray exposure is not performed.

3-2 Switching characteristics and Memory window

3-2-1 Irradiated by EUV

Fig. 3-1 shows the I-V curves of the RRAM devices before EUV irradiation and experienced different doses of EUV irradiation. Every memory device was measured right before and after irradiation. On each device, the I-V characteristics were record for ten switching cycles. The I-V curves exhibit no apparent difference. The set voltage is defined as the voltage at which the current switches from low level to high level in the set process, and the reset voltage is defined as the voltage at which the

current switches from high level to low level in the reset process. As shown in Fig. 3-1, the set voltage and the reset voltage are measured approximately 1 V and -0.8 V, respectively. No matter how high the total dose is, the set and reset voltages after irradiation are in the same range at the first ten switching cycles.

Fig. 3-2 shows the memory windows before and after EUV irradiation to different total dosages. For each total dosage, five or six devices were measured. The resistance is calculated at 0.1 V. Before irradiation, variation between devices is observed. This variation does not increase after irradiation. Similar to the switching characteristics shown in Fig. 3-1, the memory window does not change obviously by the EUV irradiation. The reason for this result is the special switching mechanism of RRAM. As discussed in section 1-3, oxygen vacancies dominate the switching characteristics of the hafnium oxide-based RRAM. The main damages in the oxide layer during irradiation are electron-hole pairs generation and bond breaking. That is, irradiation would not affect oxygen vacancies. Furthermore, the irradiation induced damages are much less than the oxygen vacancies in the oxide of RRAM after forming step. Hence, irradiation does not affect the switching characteristics and memory window.

3-2-2 Irradiated by 10keV X-ray

Fig. 3-3 show the I-V curves of the RRAM devices before and after X-ray irradiation. Similar to the results of EUV irradiation experiments, there is no apparent difference between the switching characteristics before and after X-ray irradiation even the devices received a high dose irradiation. The resistance of the high-resistance state of the RRAM devices offered by ITRI has large variation. However, there are still memory windows with resistance ratio of ~10.

3-3 Memory State and Retention Performance

3-3-1 Irradiated by EUV

Fig. 3-5 and Fig. 3-6 show the retention characteristics of RRAM devices at low-resistance state (LRS) and high-resistance state (HRS), respectively. Because the mobility of oxygen vacancy in hafnium oxide is low at room temperature, good retention performance is observed before irradiation. There is no resistance change at room temperature for 10^6 sec in either the HRS or the LRS. After irradiated by EUV, the LRS for all RRAM devices keeps at the same resistance value. Also, the retention performance does not change for additional 10^6 sec. However, for the memory devices in the HRS, some devices change their resistance value after EUV irradiation if the total dose exceeds 100 Mrads (SiO_2). The higher the total dose is, the more the devices change their resistance.

Fig. 3-7 shows the cumulative probability of the resistance before and after EUV irradiation. The LRS is stable while the resistance in HRS distributes wider and wider as the irradiation dose increases. This observation is explained by the model illustrated in Fig. 3-8. In the LRS, there are many conducting filaments in the dielectric layer. Although EUV irradiation would generate additional damages, the most parts of filaments would not be affected. Thus, the resistance of the dielectric layer would not change. On the other hand, for the RRAM devices in the HRS, the situation becomes different. In the HRS, the oxygen vacancies distribute randomly in the dielectric and do not percolate to conducting path. For the sake of the stable situation of the oxygen vacancies at room temperature, the retention performance does not change obviously. During EUV irradiation, two different situations would occur. The electron-hole pairs and broken bonds may disturb the distribution of the oxygen vacancies in the dielectric. The energy released from the recombination of high

energy electrons and holes may anneal the dielectric and reduce the defect density [38]. The current of RRAM in the HRS is conducted with both oxygen vacancies and defects in the oxide layer. Therefore, the resistance would increase if the amount of defects reduces. On the other hand, the radiation induced defects may bridge the ruptured filaments in the dielectric layer to form a conducting path. In this case, devices in the HRS may fall into LRS. The change of memory state by EUV irradiation is temporary. After a reset process, the memory device can be operated normally again. Fig. 3-9 shows an example. After irradiation, the HRS falls into LRS. In the second set/reset cycles, the LRS is reset to HRS and and the switching characteristic is kept.

3-3-2 Irradiated by 10keV X-ray

Retention performance and stability of memory states of the RRAM devices irradiated by 10 keV X-ray is shown in Fig. 3-10, Fig. 3-11, and Fig. 3-12. These results show similar trend with the devices irradiated by EUV. The retention performance does not change within 10^6 sec and the change of memory states depends on the total dose of irradiation. The devices in the low resistance state keep the same state no matter how high the total dosage is, while the devices in the high resistance state may change their resistance when the total dose is over 600 Mrads (SiO_2). Also, in this experiment we can also see the fact that radiation affects the dielectric layers in two different ways. On one hand, radiation anneals the dielectric layer, raising the resistance; on the other hand, radiation generated defects bridging the filaments, and then lowering the resistance.

3-4 Endurance Performance

The endurance performance of RRAM changes from device by device, and the

endurance test is destructive. Thus, thirty different devices are measured before and after irradiation. Each device is operated at the same set and reset conditions as those used in the switching characteristics measurement for two thousand cycles. Table 3-1 shows the three typical results. The device in Fig. 3-13 (a) operates normally after two thousand cycles. The resistance ratio does not change. The device in Fig. 3-13 (b) can not be reset to HRS after two thousand cycles operation. The resistance ratio diminishes to one. The resistance ratio of the device in Fig. 3-13 (c) decreases to be lower than ten after two thousand cycles operation. Here we define the device failure as the resistance ratio of the device decreases to be lower than 10. That is the devices in Fig. 3-13 (b) and (c). The percentage of the failed devices for the non-irradiated samples is about 33 %.

The selected total doses are 1 Mrads (SiO_2), 600 Mrads (SiO_2), and 900 Mrads (SiO_2). The dose of 1 Mrads (SiO_2) is to compare with the published results using gamma ray as the irradiation source [31]. The reason for choosing 600 and 900 Mrads (SiO_2) is because only in these doses the memory state changes. For each dose, eight devices were measured. The failure percentage is listed in Table 3-2. The failure percentages for the total dose of 1 Mrads (SiO_2), 600 Mrads (SiO_2), and 900 Mrads (SiO_2) are 12 %, 50 %, and 62 %, respectively. The number of failed devices increases with the increase of total dose. The oxide layer will induce lots of defects through plenty of switching cycles, leading to oxide breakdown. Thus, the failure is permanent. The HRS can not be reset by the typical operation condition.

3-5 Difference between EUV and X-ray Irradiation

According to the results in the previous three sections, it is observed that EUV and X-ray irradiations have similar effects on the RRAM characteristics. However, it

seems that RRAM is more immune to X-ray than EUV. The change of memory state is observed when the total dose of EUV increases to 100 Mrads (SiO_2); however, it is not observed until the total dose increases to 600 Mrads (SiO_2) for the devices irradiated by X-ray. This difference can be explained from two points of view.

First, the attenuation length in hafnium oxide for the EUV which has the energy of 91.85 eV is different from the 10 keV X-ray. Fig. 3-14 shows the attenuation length of EUV and X-ray, respectively. From the attenuation length we can have the penetration probability by the formula $P(x) = e^{-\frac{x}{\lambda}}$, where P is the penetration probability, λ is the attenuation length, and x is the thickness of oxide which is 5 nm in this thesis. The penetration probabilities are 0.846 for the EUV and 0.999 for the X-ray, which means the absorption rate is 0.154 for the EUV and 0.001 for the X-ray. Since the energy of X-ray is about 109 times higher than that of EUV, the total energy absorbed by the 5-nm-thick hafnium oxide during EUV irradiation is about 1.41 times stronger than that during 10 keV X-ray irradiation. Hence, for the same flux, the effect arising from EUV is lightly stronger than that from 10 keV X-ray. On the other side, as the definition of the total dose discussed in section 2-5, the formula contains both the energy and flux of the irradiation. Therefore, even the total dose are in the same value for EUV and 10 keV X-ray, for example, both in 900 Mrads (SiO_2), the total flux of EUV is about 109 times higher than that of 10 keV X-ray because of the difference in energy. Hence, from the above two points, the effect of EUV is stronger than that of X-ray on RRAM devices.

3-6 Summary

The effect of EUV and 10 keV X-ray irradiation induced damages on the characteristics of RRAM devices are investigated.

For the switching characteristics and memory windows of RRAM, radiation does not much damage on the RRAM devices. This is because the switching process of RRAM contains the recombination of the oxygen vacancies. During this trapping and detrapping process, the defects induced by radiation which might affect the conduct filaments in the oxide at first would be partly canceled out. Hence, even there are defects induced by radiation in the oxide, the switching process is not affected. Besides, the defects induced by radiation are less than that in the oxide which is after forming process. Therefore, the value of high and low resistance during switching; that is, memory window keeps at almost the same window as that before irradiation.

After irradiation, the retention characteristics show the same way as that before irradiation, even for EUV or X-ray. The results could be explained by the fact that the oxygen vacancies almost don't move in the room temperature. Thus, the conducting filaments would not be affected, keeping the resistance of a device in the same value. However, for the devices already have the memory state stored, there are some chances that the stored memory state might change, especially for the devices with high total dose. Devices irradiated by EUV lose the memory state once the total dose over 100 Mrads (SiO_2), while devices irradiated by X-ray have the issue of losing stored state over 600 Mrads (SiO_2). The different levels of damage between two sorts of radiation is because the different attenuation length on the hafnium oxide and the definition of the total dose. Because the total dose used here contains the contribution of energy and flux, and both of them are proportional to the value of total dose. Thus, the process of calculation will make the flux for X-ray less than that for EUV. Besides, even in the situation of same flux, the total energy absorbed in the oxide for the X-ray is also less than that for the EUV, because of the different attenuation length.

The endurance performance degrades after high total dose irradiation by X-ray. This shows that radiation indeed induces damage on oxide. However, this damage is

global in the oxide. Therefore, in few numbers of switching cycles, the effects of damage would not be observed. Nevertheless, after thousands of switching cycles, the oxide layer in a stress situation. Thus the defects that not influence the characteristics at first might induce hard breakdown in this situation. Thus, if there are more enough defects in the oxide, the endurance performance might degrade.

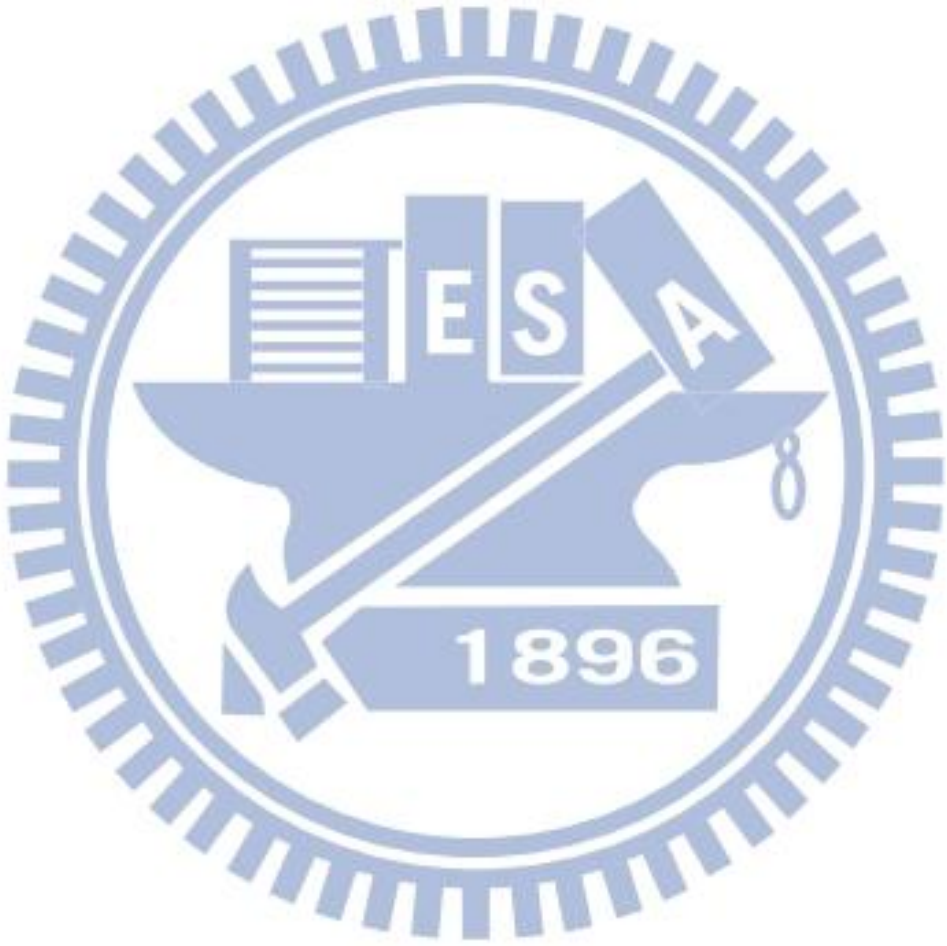

Table 3-1: Proportion of failed devices before irradiation and after different total dose irradiation

	Pre irradiation	1 Mrads (SiO_2)	300 Mrads (SiO_2)	600 Mrads (SiO_2)
Failed percentage (%)	33	12	50	62

Table 3-2: Comparison between devices irradiated by EUV and X-ray

	Switching characteristics	Memory windows	Retention
EUV	No change	No change	No change
X-ray	No change	No change	No change

	Memory state	Endurance
EUV	Change over 100 Mrads (SiO_2)	
X-ray	Change over 600 Mrads (SiO_2)	Change over 600 Mrads (SiO_2)

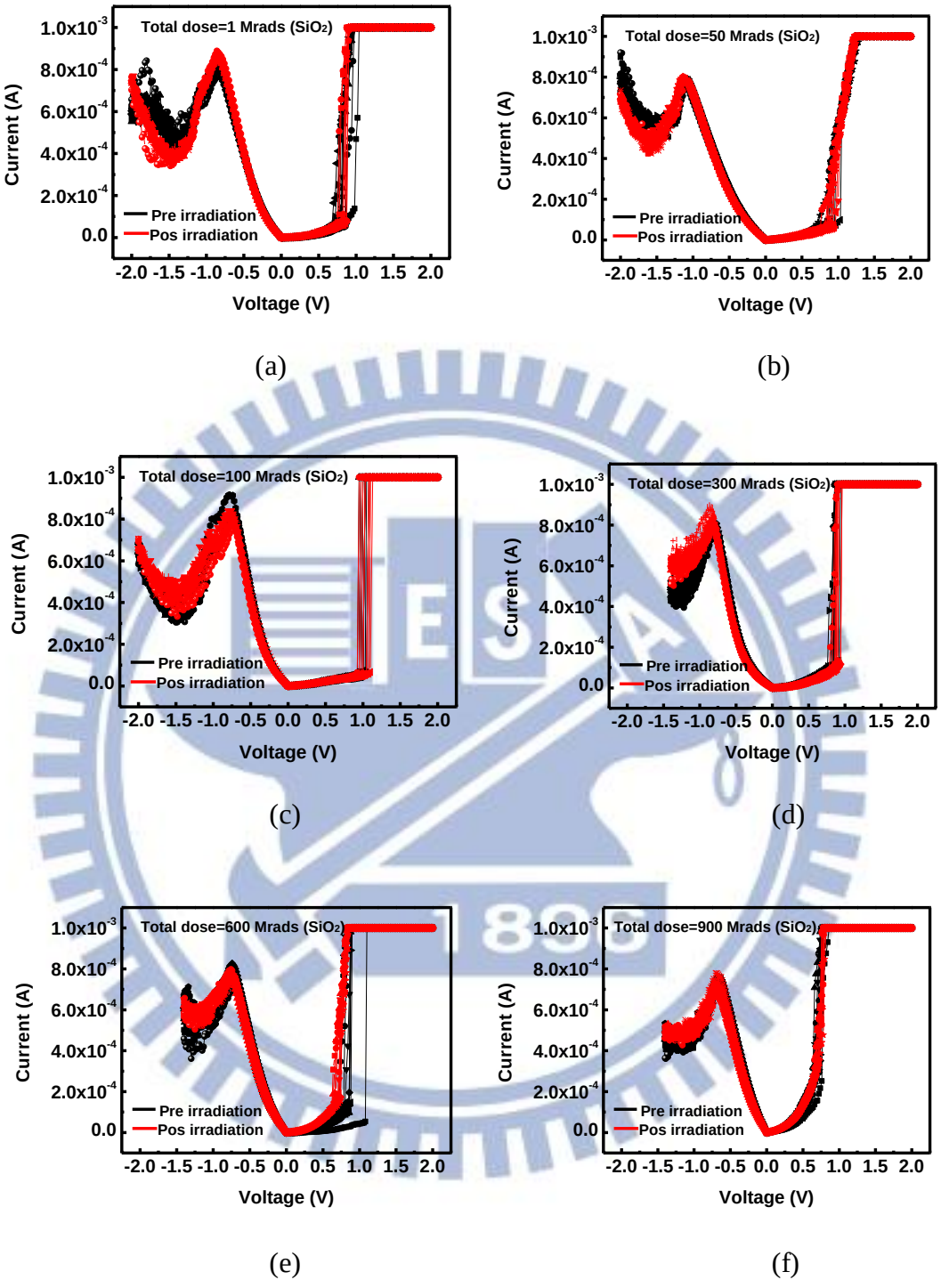

Fig. 3-1: I-V curves for the RRAM devices irradiated by EUV with different total dose, all devices are switched ten cycles before and after the irradiation

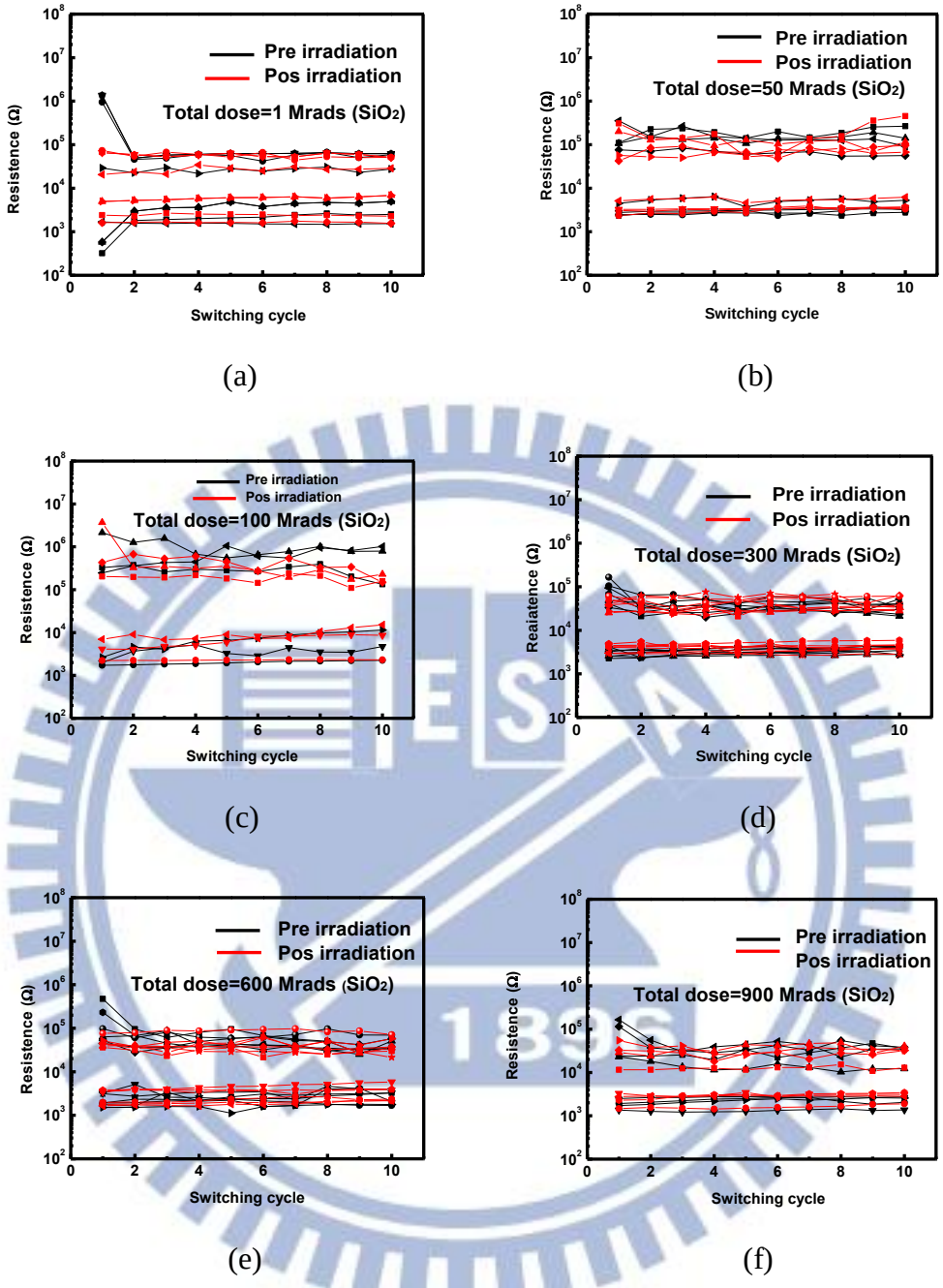

Fig. 3-2: Memory windows for the RRAM devices irradiated by EUV with different total dose, all devices are switched ten cycles before and after the irradiation

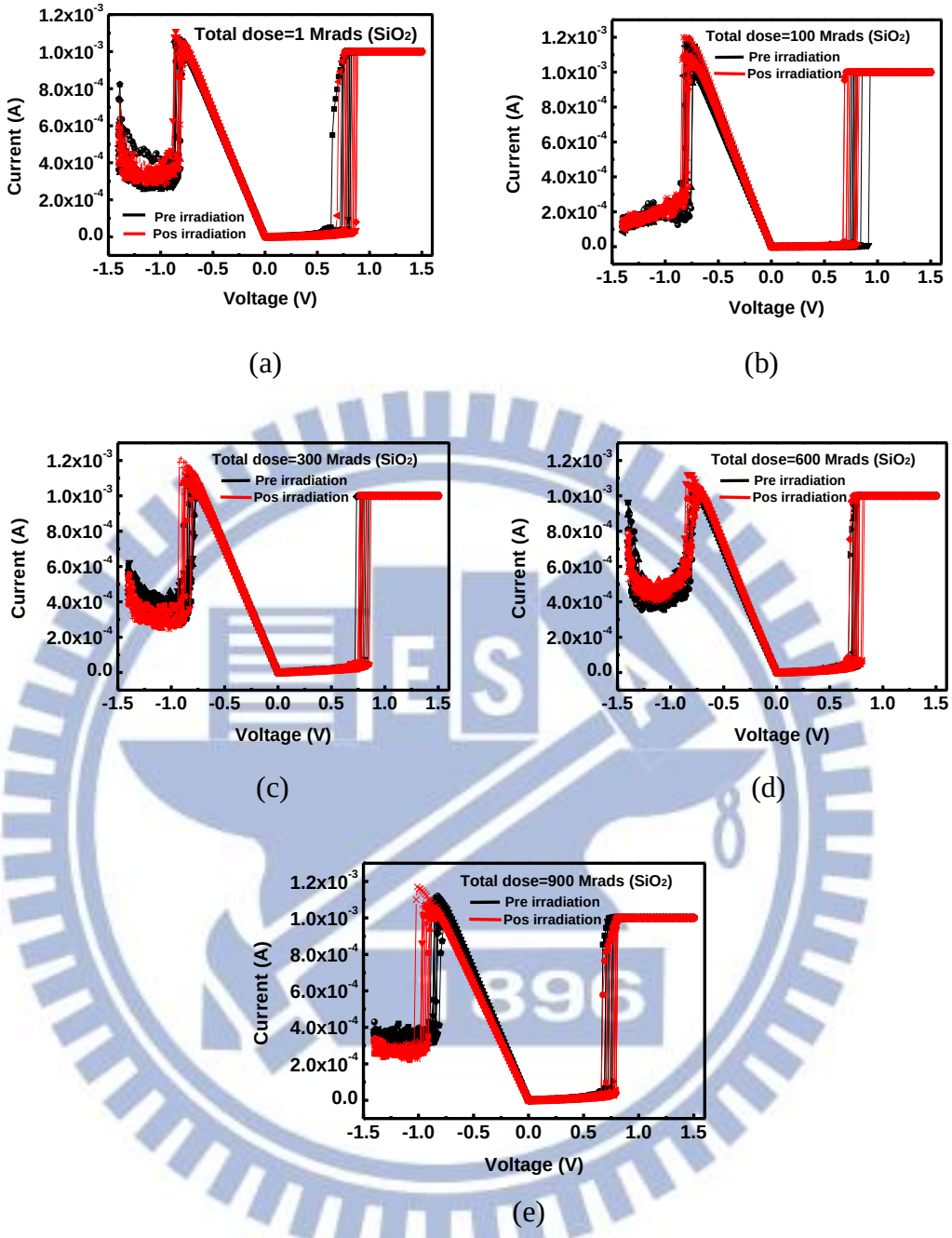

Fig. 3-3: I-V curves for the RRAM devices irradiated by X-ray with different total dose, all devices are switched ten cycles before and after the irradiation

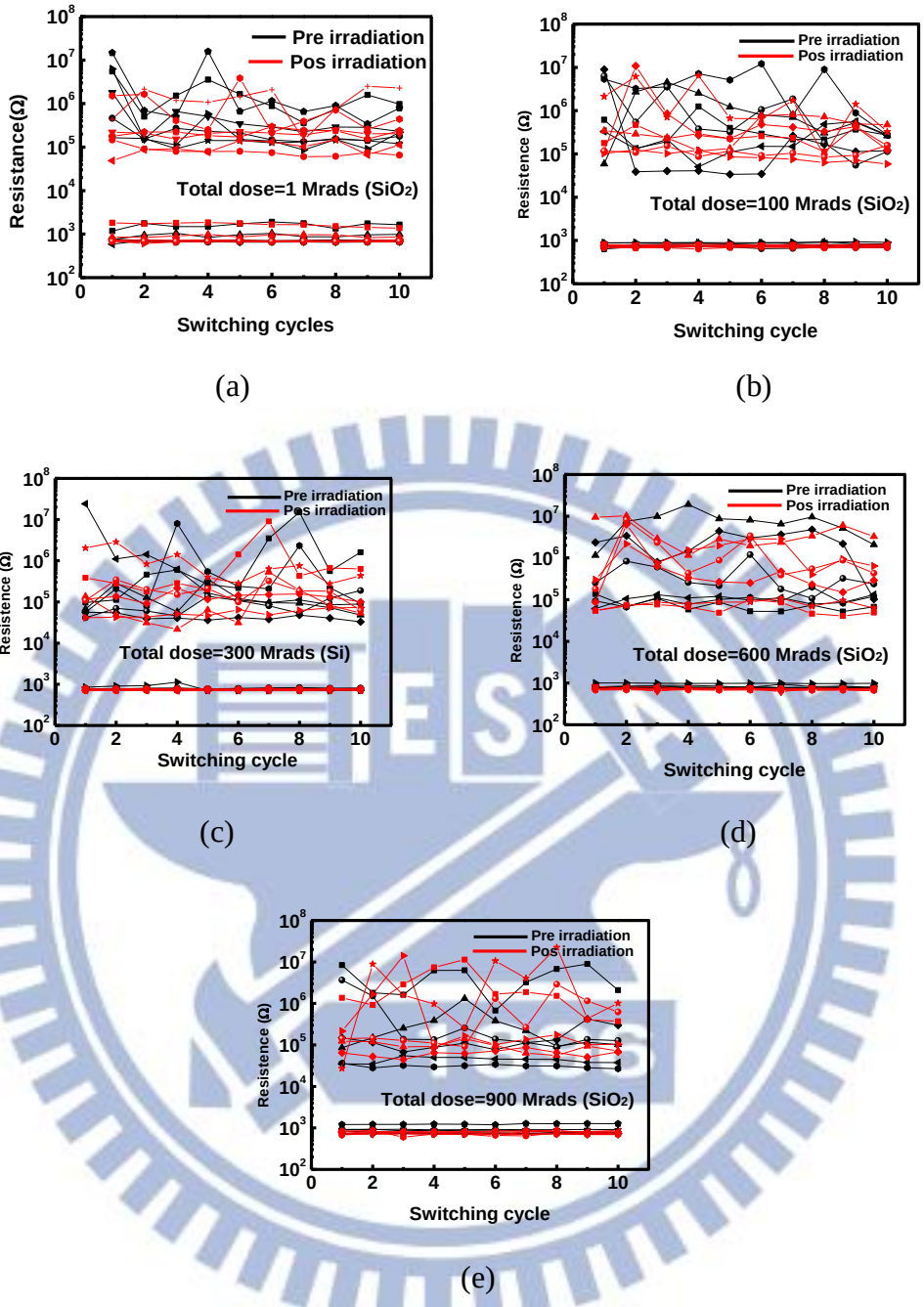

Fig. 3-4: Memory windows for the RRAM devices irradiated by X-ray with different total dose, all devices are switched ten cycles before and after the irradiation

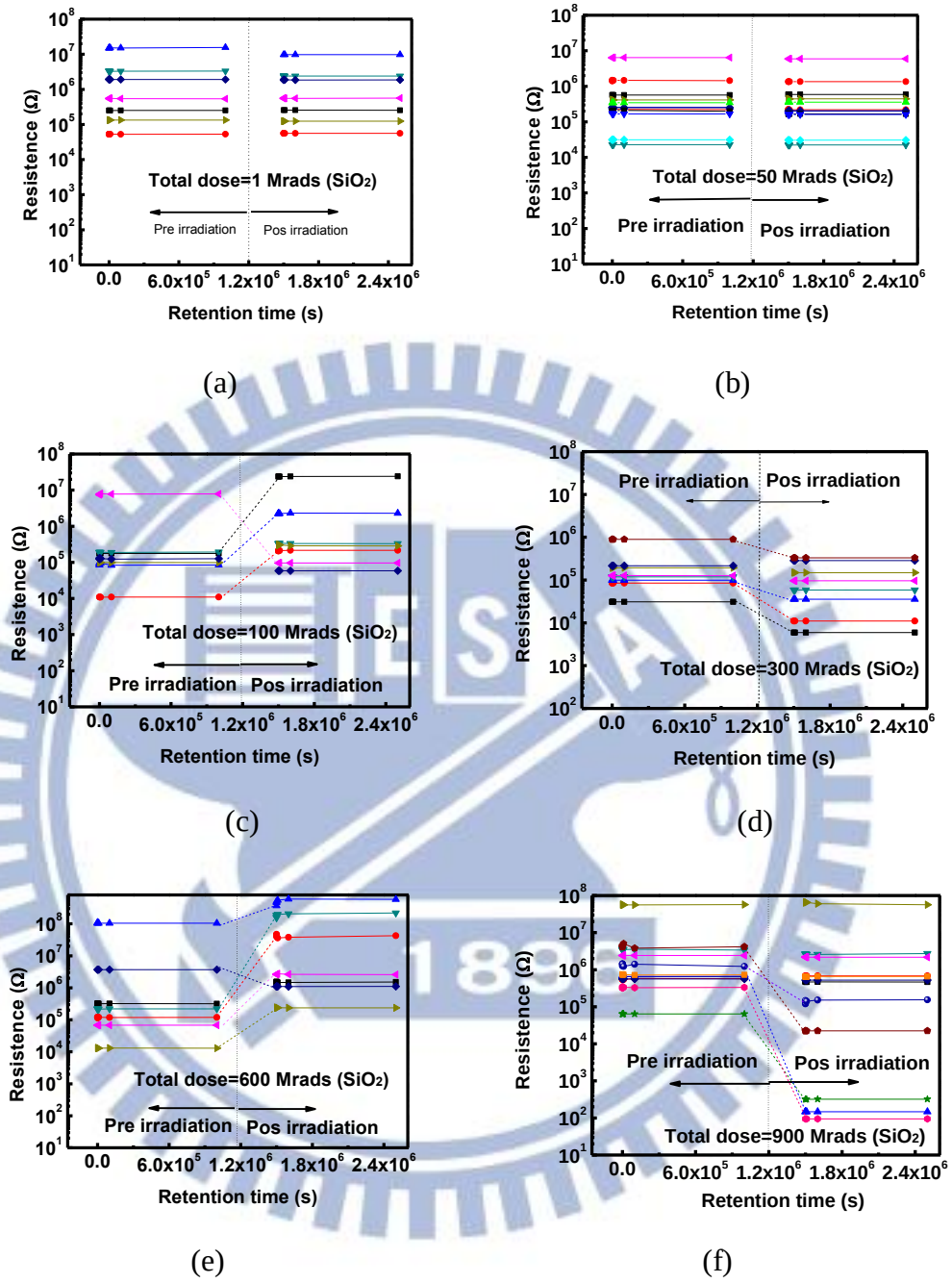

Fig. 3-5: Retention characteristics for the RRAM devices set at the high resistance state and irradiated by EUV with different total dose, the dot lines in the pictures are just for the devices having memory state changing

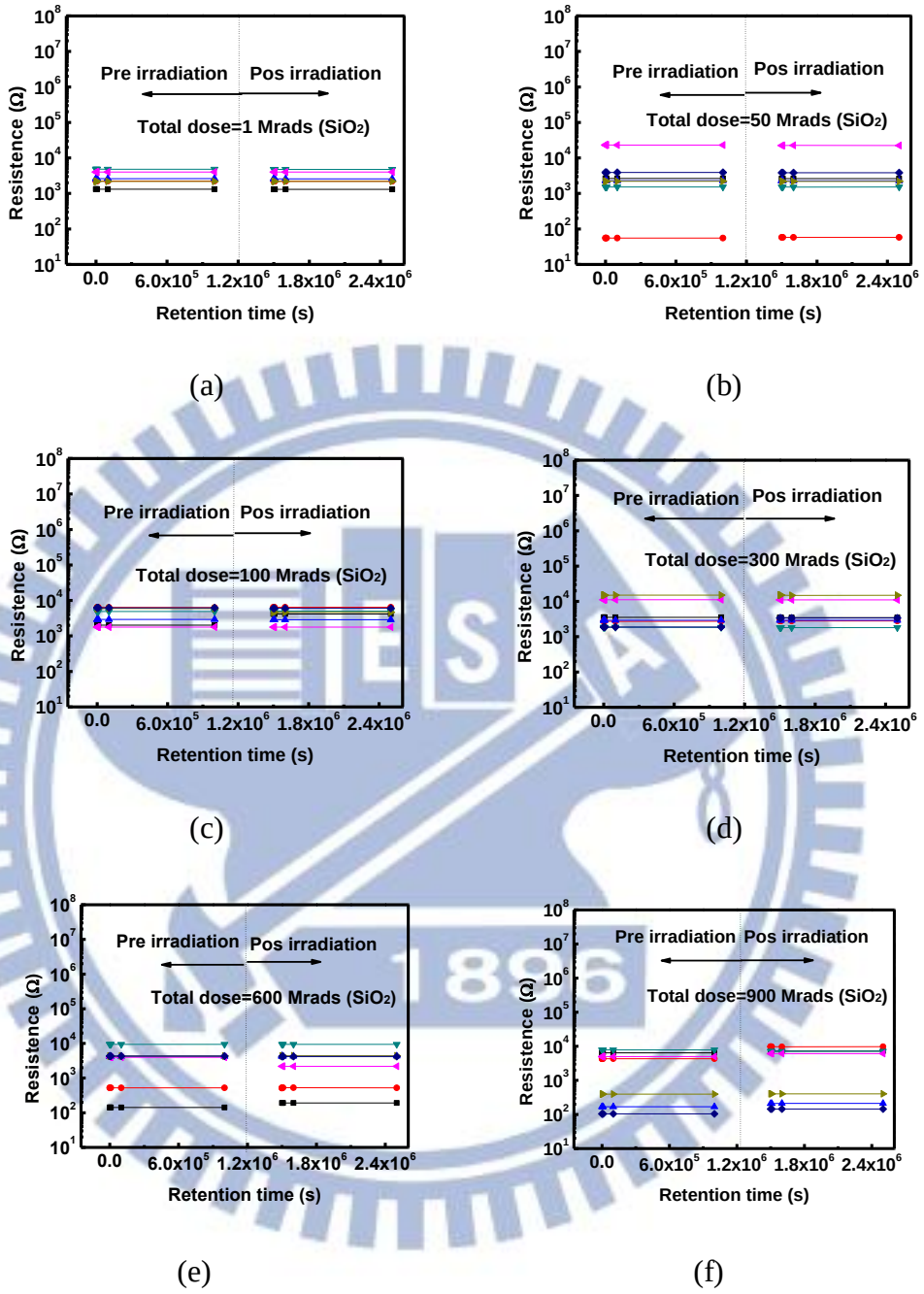

Fig. 3-6: Retention characteristics for the RRAM devices set at the low resistance state and irradiated by EUV with different total dose, the dot lines in the pictures are just for the devices having memory state changing

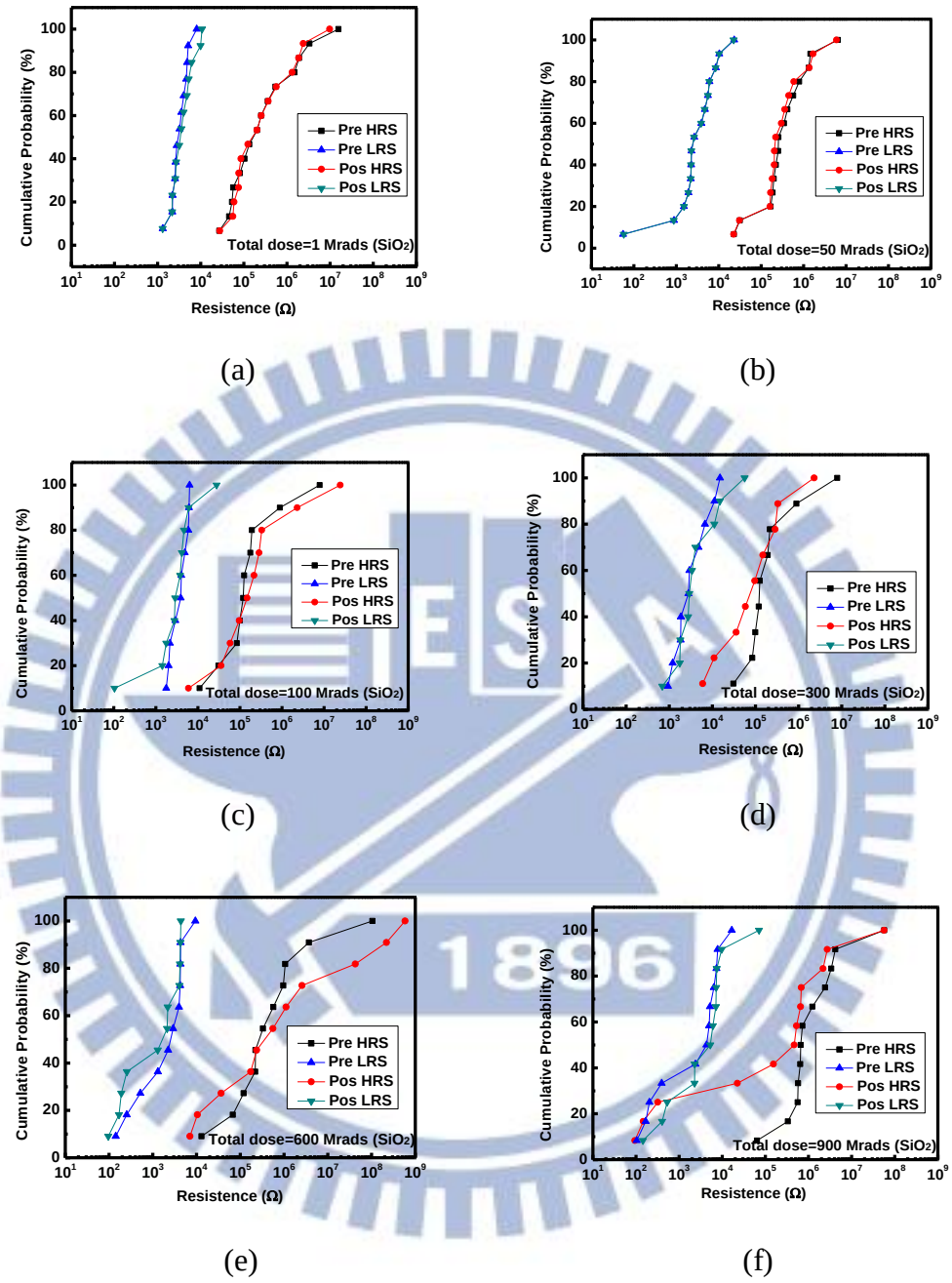

Fig. 3-7: The cumulative probability plots for the RRAM devices irradiated by EUV with different total dose.

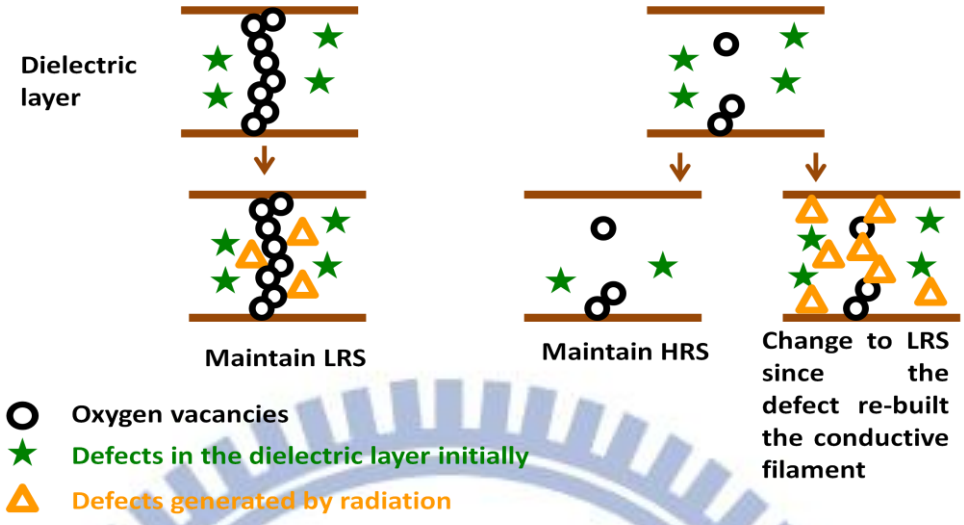

(a) (b)

Fig. 3-8: (a) Devices initially at low resistance state have conducting filaments composed with lots of oxygen vacancies all over the oxide layer. Even there are defects induced by radiation, the still keep in low resistance state.

(b) Devices initially at high resistance state have few broken conducting filaments in the oxide layer. The defects induced by radiation have a chance to repair the conducting filaments, making the device change into low resistance state.

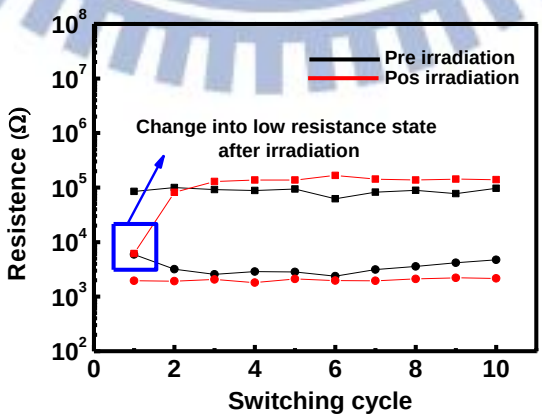

Fig. 3-9: The device changing into low resistance after irradiation reset to high resistance in the switching process

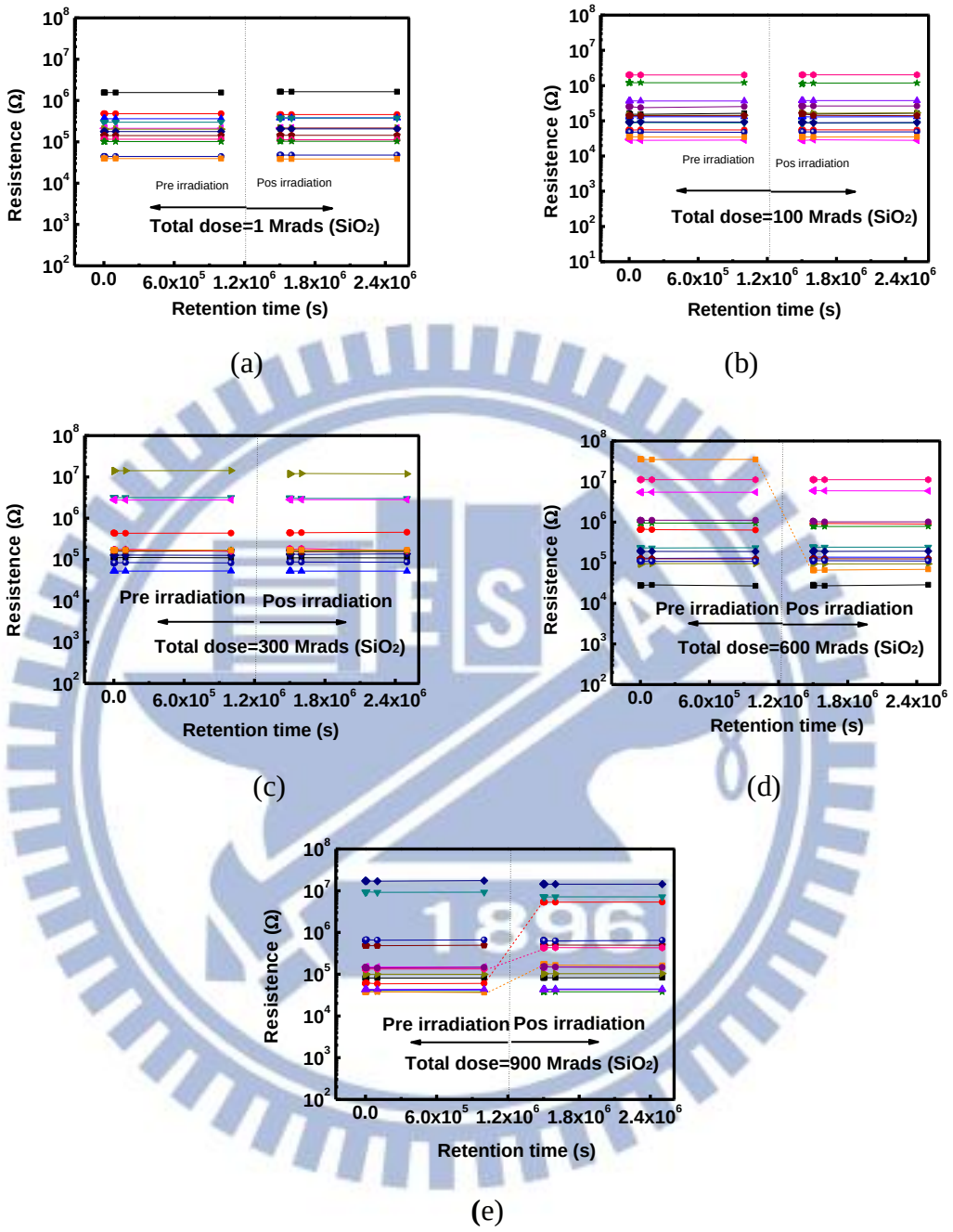

Fig. 3-10: Retention characteristics for the RRAM devices set at the high resistance state and irradiated by EUV with different total dose, the dot lines in the pictures are just for the devices having memory state changing

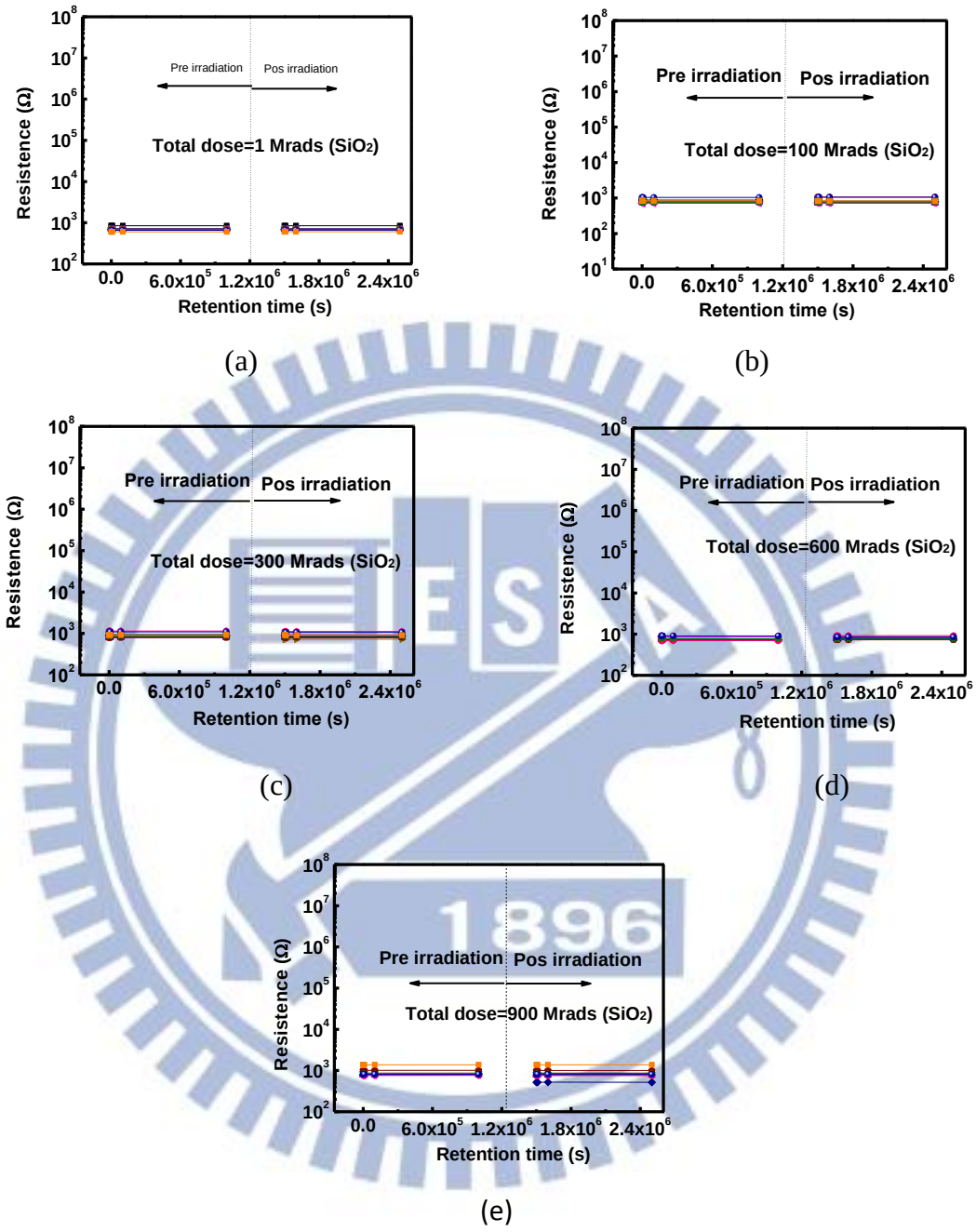

Fig. 3-11: Retention characteristics for the RRAM devices set at the low resistance state and irradiated by X-ray with different total dose, the dot lines in the pictures are just for the devices having memory state changing

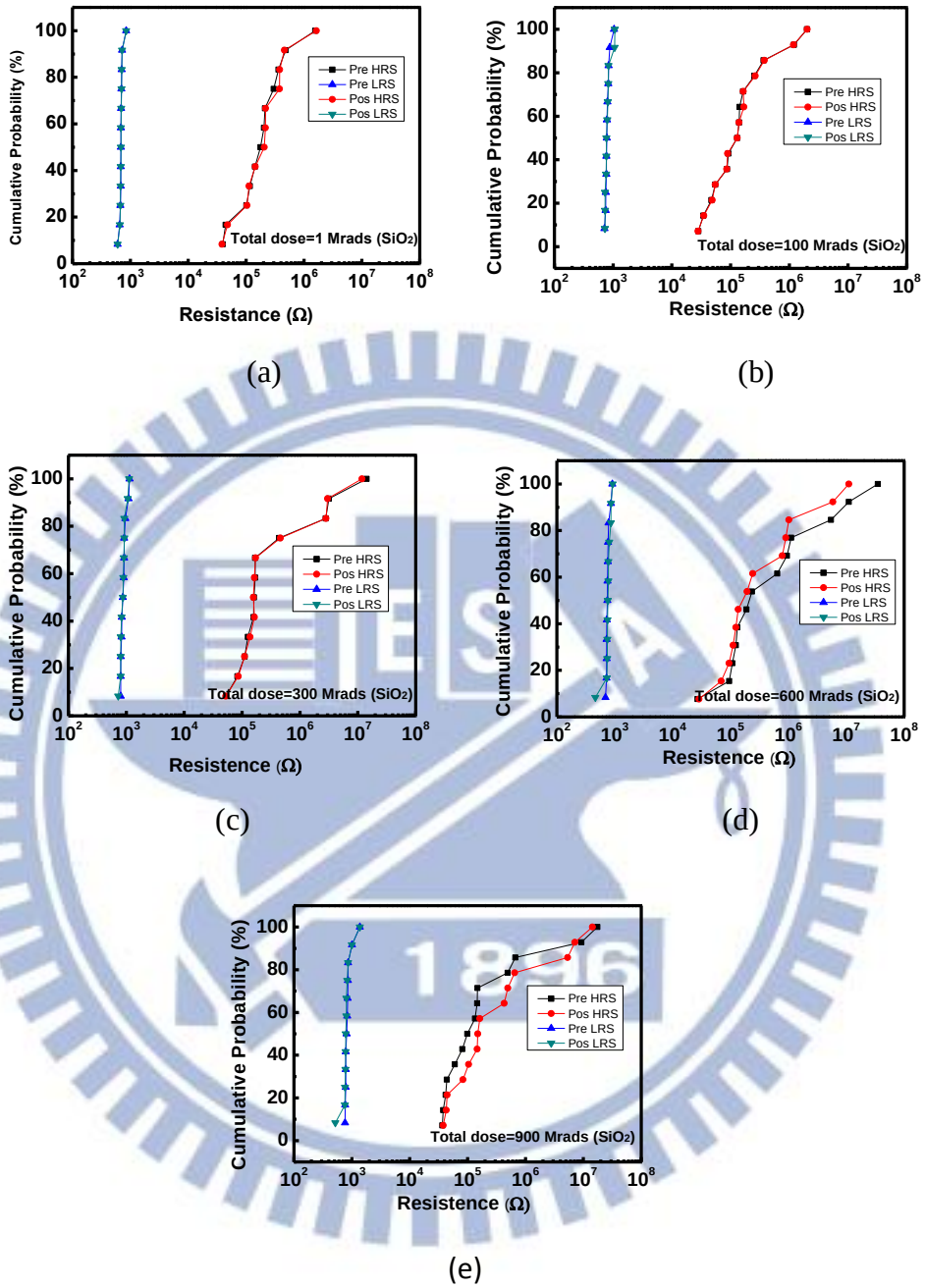

Fig. 3-12: The cumulative probability plots for the RRAM devices irradiated by X-ray with different total dose.

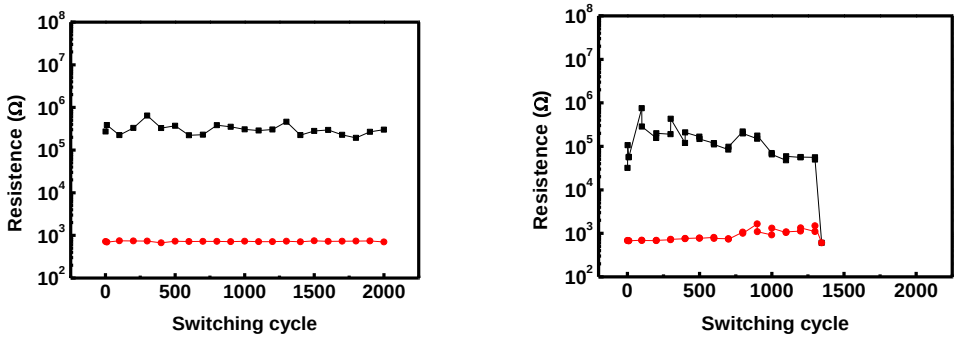

(a) (b)

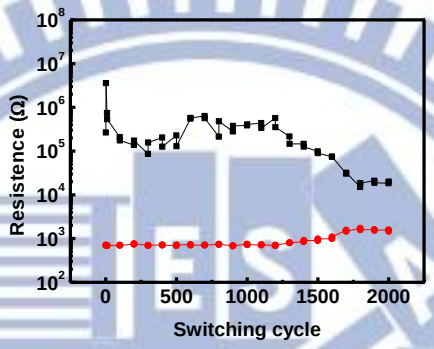

(c)

Fig. 3-13: (a) Devices can switch over two thousands cycles

(b) Devices can't switch over two thousands cycles

(c) Devices have window less than ten times between high and low resistance state

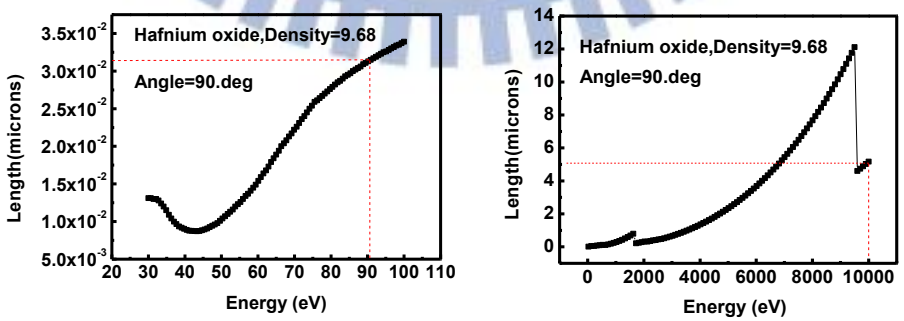

(a) (b)

Fig. 3-14: (a) Attenuation length for EUV on hafnium oxide

(b) Attenuation length for X-ray on hafnium oxide

Chapter 4
Conclusions and Future Works

4-1 Conclusions

In this thesis, the impact of EUV and X-ray irradiation induced damages on the characteristics of RRAMs was studied. The EUV is used for the reason that the EUV lithography is a promising next generation lithography technology, and once occurs, the radiation damage induced by EUV on the performance of RRAM is an important issue. According to our experiments, on the RRAM cells irradiated by EUV, the switching characteristics, memory window, and retention performance have no obvious degradation phenomena. The main reasons are correlated to the operation mechanism of RRAM. At first, the RRAM change its memory states between 0 state and 1 state through the migration of oxygen vacancies for the hafnium oxide based RRAM. The primary damage from irradiation, the generation of electron-hole pairs, does not affect the oxygen vacancies. Besides, the amount of defects generated by irradiation is much less than that of oxygen vacancies in dielectric. Therefore, the switching characteristics and memory windows are not change. The mobility of oxygen vacancies is low at room temperature, leading to good retention performance of RRAM, even after irradiation. The change of the stored memory state is also measured. RRAM cells are set to high resistance state (HRS) and low resistance state (LRS) before irradiation, and be measured right after irradiation. The cells in the LRS have no resistance change after irradiation, no matter how much the total dose is. On the other hand, some cells originally in the HRS change their resistance through the irradiation, and the number of failed cells increases with the total dosage. This is owing to the fact that there are few oxygen vacancies in the oxide layer for the cells in the HRS. In this condition, radiation has two sorts of effects on the oxide layer,

annealing and defects generation. The annealing of oxide layer will make the resistance higher, while the generation of defects might re-bridge the broken filaments, leading to the resistance lowering. In the worst case, the memory state may change to the LRS. On the other hand, there are several filaments in the oxide layer for the cells in the LRS. Therefore, even some of filaments are interrupted by the high energy radiation, there are still enough filaments keeping the cell in the LRS. The cells changing state from HRS to LRS after radiation exposure are able to be reset back to the HRS and switching normally again, implying the switching process will repair the radiation induced defects.

On the other hand, the 10 keV X-ray is used to study the effect of the energy of the radiation source. RRAM cells irradiated by X-ray show almost the same trend as those irradiated by EUV. The characteristics of memory window, switching performance, and retention performance have no degradation through the high dose X-ray exposure. However, a large number of the cells in the HRS are failed once the total dose of the X-ray increases to 600 Mrads (SiO_2). Similar to the result in the EUV experiment, the high total dose irradiation will induce enough number of defects to affect the oxide layer. Also, the two tendencies of resistance variation are observed, implying that the radiation might anneal the oxide or induce defects to connect the filaments, lowering the resistance.

The endurance performance is tested in the X-ray experiment. The high total dose of X-ray over 600 Mrads (SiO_2) indeed degrades the endurance performance of almost half of the tested cells, while the low total dose of 1 Mrads (SiO_2) X-ray almost does not affect the endurance performance. The failed cells which finally in the LRS can not be reset back to the HRS. This result implies that defects induced by radiation are not repaired through the switching process might induce oxide breakdown. Therefore, the degradation of the endurance performance depends on the

total dose. The different levels of damage generated by EUV and X-ray is because the calculation method of the total dose we used. The total dose is proportional to the energy and flux of light; thus, the flux of X-ray is much less than that of EUV at the same total dose. Hence, the damage by EUV on RRAM is heavier than that by X-ray.

The radiation damage research of EUV on the SONOS and nano-crystal memory has been studied. The SONOS device has several degradations after EUV, including memory window, retention performance, and endurance. The memory window can be recovered automatically after few days, while the endurance degrades very hard and can't be recovered through medium temperature annealing. For the nano-crystal memory, almost all the performances are not affected by the EUV radiation, existing great immunity to EUV. In this study of RRAM irradiated by EUV, the memory window and retention performance are not affected by EUV. Even if the stored memory state will be disturbed in high total dose, the memory state can be recovered through a normal switching process. Hence, whether in the lithography or operation environment, the RRAM has good radiation hardness against EUV.

On the RRAM irradiated by X-ray, except the stored state changing, the endurance also degrades in high total dose. However, for the high energy radiation environment, the regular total dose is around 0.1 Mrads (SiO_2) to 1 Mrads (SiO_2). Therefore, if the total dose is not too high, RRAM still shows good immunity to X-ray.

4-2 Future Works

At first, the oxide of the RRAM can be made thicker. The oxide layer in this work is 5 nm, which is too thin to observe the radiation damage effect, as discussed in chapter 3. Second, we realize that the RRAM used in the EUV experiment is not as

good performance as the RRAM fabricated by industry, especially for the endurance performance. Therefore, high performance RRAM should be used to double confirm the results in this work. Besides, the sample size in this thesis is too small. More devices should be tested. Furthermore, the failed cells in the endurance test can be tested in the test of retention performance first. Thus, we can find that whether the cell has endurance degradation also has the stored state lost issue, confirming more clearly the reason for the endurance degradation. On the other hands, stress test after irradiation with the voltage in normal switching process should be studied. By this test, we can also confirm the mechanism of endurance degradation after irradiation. Finally, the MIM structure of Hafnium oxide-based should also be tested. Because the measurement of MIM capacitor can know the trap in the oxide layer, it is able to clarify the radiation damage effect on the MIM capacitor.

References

[1] B. Wuand, and A. Kumar, "Extreme ultraviolet lithography: A review," *J. Vac. Sci. Technol. B* , vol. 25,no. 6, pp. 1743-1761, Nov. 2007.

[2] J. E. Bjorkholm, "EUV Lithography—The Successor to Optical Lithography?" *Intel Tech. J.*, vol. 2, no. 3, 1998.

[3] C. W. Gwynb, R. Stulen, D. Sweeney, and D. Attwood, "Extreme ultraviolet lithography," *J. Vac. Sci. Technol. B* , vol. 16, no. 6, pp. 3142-3149, Nov. 1998.

[4] C. Vieu, , F. Carcenac1, A. Pépin, Y. Chen, M. Mejias, A. Lebib, L. Manin-Ferlazzo, L. Couraud, H. Launois, "Electron beam lithography: resolution limits and applications" *Applied Surface Science*, vol. 164, no. 1–4, pp. 111–117, Sep. 2000.

[5] K. Kemp and S. Wurm, "EUV lithography," *C. R. Phys.*, vol. 7, no. 8, pp. 875–886, Oct. 2006.

[6] P. J. Silverman, "Extreme ultraviolet lithography: overview and development status" *J. Microlith., Microfab., Microsyst.*, vol.4, no. 1, p. 011006, Mar. 2005.

[7] S. Schröder, T. Feigl, A. Duparré, and A. Tünnermann1, "EUV reflectance and scattering of Mo/Si multilayers on differently polished substrates" *Optics Express*, vol. 15, no. 21, pp. 13997-14012, 2007

[8] B. J. Rice, V. Jindal, C.C. Lin, J. Harris-Jones, H. Kwon, A. Ma, M. Goldstein, F. Goodwin, "Overview of Mask Metrology" *AIP Conf. Proc.*, vol. 1395, 2011, pp.281-289.

[9] Luke Collins, "TSMC joins Intel as ASML investor to accelerate availability of EUV, 450 mm lithography" *Tech Design Forum*, Posted: August 6, 2012

[10] T. P. Ma and Paul V. Dressendorfer, "Ionizing radiation effects in MOS devices and circuits," Wiley, New York, 1996.

[11] J. A. Felix, J. R. Schwank, C. R. Cirba, R. D. Schrimpf, M. R. Shaneyfelt, D. M. Fleetwood and P. E. Dodd, "Influence of total-dose radiation on the electrical characteristics of SOI MOSFETs," *Microelectronic Engineering*, vol. 72, no. 1-4, pp. 332-341, 2004.

[12] S. K. Dixit, X. J. Zhou, R. D. Schrimpf, D. M. Fleetwood, S. T. Pantelides, R. Choi, G. Bersuker, and L. C.Feldman, "Radiation induced charge trapping in ultrathin HfO_2-based MOSFETs," *IEEE Trans. Nuc. Sci*, vol. 54, no. 6, pp. 1883-1890, Dec. 2007.

[13] J. A. Felix, M. R. Shaneyfelt, D. M. Fleetwood, T. L. Meisenheimer, J. R. Schwank, R. D. Schrimpf, P. E. Dodd, E. P. Gusev, and C. D'Emic, "Radiation-Induced Charge Trapping in Thin $Al_2O_3/SiO_xN_y/Si$ (100) Gate Dielectric Stacks," *IEEE Trans. Nucl. Sci.*, vol. 50, no. 6, pp. 1910-1918, Dec.2003.

[14] G. Cellere, A. Paccagnella, S. Lora, A. Pozza, G. Tao, A. Scarpa, "Charge Loss After ^{60}Co Irradiation of Flash Arrays," *IEEE Trans. Nucl. Sci.*, vol. 51, no. 5, pp. 2912-2916, Oct. 2004.

[15] N. Wrachien, A. Cester, R. Portoghese, and C. Gerardi, "Investigation of Proton and X-Ray Irradiation Effects on Nanocrystal and Floating Gate Memory Cell Arrays," *IEEE Trans. Nucl. Sci.*, vol. 55, no. 6, pp. 3000-3008, Dec. 2008.

[16] T. R. Oldham, M. Suhail, P. Kuhn, E. Prinz, H. S. Kim, and K. A. Label, "Effects of Heavy Ion Exposure on Nanocrystal Nonvolatile Memory," *IEEE Trans. Nucl. Sci.*, vol. 52, no. 6, pp. 2366-2371, Dec. 2005.

[17] C. C. Yen, "Effect of Extreme Ultra-Violet Radiation on Advanced Non-volatile Memories" *Master thesis*, National Chiao Tung University, Department of Electronics Engineering, 2010.

[18] C. Y. Lu, K. Y. Hsieh, and R. Liu, "Future challenges of flash memory

technologies," *Microelectronic Engineering.*, vol. 86, no. 3, pp. 283-286, Mar. 2009.

[19]G. Atwood, "Future directions and challenges for ETox flash memory scaling," *IEEE Trans. Device Mater.Rel.* , vol. 4, no. 3, pp. 301-305, Sept. 2004

[20] G. Hu, P. L. Trouilloud, D. W. Abraham, S. Brown, M. C. Gaidis, J. Nowak, E. J. O'Sullivan, R. P. Robertazzi, J. Z. Sun, W. J. Gallagher, "Switching distributions and write reliability of perpendicular spin torque MRAM", in *IEDM Tech. Dig.*, 2010, pp. 12.5.1 - 12.5.4

[21] G. Servalli, "A 45 nm generation Phase Change Memory technology", in *IEDM Tech. Dig.*, 2009, pp. 1-4

[22] S. I. Kim, J. H. Lee, Y. W. Chang, S. S. Hwang, and K. H. Yoo, "Reversible resistive switching behaviors in NiO nanowires", *Appl. Phys. Lett.* vol. 93, no. 3, p. 033503, Jul. 2008

[23]T. Perez and C. A. F. De Rose, "Non-Volatile Memory: Emerging Technologies And Their Impacts on Memory Systems", *Technical Report*, Pontifical Catholic University, Faculty of Computer Science, 2010.

[24] J. Y. Son, Y. H. Shin, H. Kim, and H. M. Jang, "NiO Resistive Random Access Memory Nanocapacitor Array on Graphene" *ACS Nano.*, vol. 4, no. 5, pp. 2655-2658, 2010.

[25] H. Y. Jeong, Y. I. Kim, J. Y. Lee, and S. Y. Choi, "A low-temperature-grown TiO_2-based device for the flexible stacked RRAM application" *Nanotechnology* vol. 21, no.11, p. 115203, Feb. 2010.

[26] Y. Wu, "Ultra-low power Al_2O_3-based RRAM with 1μA reset current", in *Proc. of VLSI-TSA*, 2010, pp. 136-137.

[27] S. Y. Wang, D. Y. Lee, T. Y. T, and C. Y. Lin, "Effects of Ti top electrode thickness on the resistive switching behaviors of rf-sputtered ZrO_2 memory

films", *Appl. Phys. Lett*. vol. 95, no. 11, p.112904, Sep. 2009

[28] P. Y. Gu, Y. S. Chen, H. Y. Lee, P. S. Chen, W. H. Liu, W. S. Chen, Y. Y. Hsu, F. Chen, and M. J. Tsai. "Scalability with silicon nitride encapsulation layer for Ti/HfO_x pillar RRAM", in *Proc. of VLSI-TSA*, 2010, pp. 146-147.

[29] S. T. Hsua and T. Li. "Resistance random access memory switching mechanism", *J. Appl. Phys.*, vol.101, no.2, p. 024517, Jan. 2007

[30] Po-Hsueh Li, "Effect of Extreme Ultra-Violet Radiation on High Dielectric Constant Dielectrics", *Master thesis*, National Chiao Tung University, Department of Electronics Engineering, 2010.

[31] Y. Wang, H. Lv, W. Wang, Q. Wang, Z. Huo, S. Zhang, Y. Li, Q. Zuo, W. Lian, J. Yang, and M. Liu, "Highly Stable Radiation-Hardened Resistive-Switching Memory", *IEEE Electron Device Lett*, vol. 31, no. 12, pp. 1470-1472, Dec. 2010

[32] L. Zhang, R. Huang, D. Gao, P. Yue, P. Tang, F. Tan, Y. Cai, and Y. Wang, "Total Ionizing Dose (TID) Effects on TaO_x-Based Resistance Change Memory", *IEEE Trans, Electron Devices,* vol. 58, no. 8, pp. 2800 – 2804, Aug. 2011

[33] H. Y. Lee, P. S. Chen, T. Y. Wu, Y. S. Chen, C. C. Wang, P. J. Tzeng, C. H. Lin, F. Chen, C. H. Lien, and M.-J. Tsai, "Low Power and High Speed Bipolar Switching with A Thin Reactive Ti Buffer Layer in Robust HfO_2 Based RRAM" in *IEDM Tech. Dig.*,2008, pp. 1–4

[34] Y. S. Chen , T. Y. Wu, P. J. Tzeng, P. S. Chen, H. Y. Lee, C. H. Lin, F. Chen, M. J. Tsai, "Forming-free HfO_2 bipolar RRAM device with improved endurance and high speed operation", in *Proc. of VLSI-TSA, 2009*, pp. 37–38.

[35] D. C. Gilmer, G. Bersuker, H-Y. Park, C. Park, B. Butcher, W. Wang, P. D. Kirsch, and R. Jammy, "Effects of RRAM Stack Configuration on Forming Voltage and Current Overshoot" in *Proc. IMW, Conf.*, 2009, pp. 1–4.

[36] H. J. Wan, P. Zhou, L. Ye, Y. Y. Lin, T. A. Tang, H. M. Wu, and M. H. Chi, "In

Situ Observation of Compliance-Current Overshoot and Its Effect on Resistive Switching" *IEEE Electron Device Lett.*, vol. 31, no. 3, pp. 246-248, Mar. 2010

[37] C. Z. Zhao, S. Taylor, M. Werner, P. R. Chalker, R. J. Potter, J. M. Gaskell and A. C. Jones, "High-k materials and their response to gamma ray radiation," *J. Vac. Sci. Technol. B*, vol. 27, no. 1, pp. 411-415, Jan. 2009.

[38] J. T. Ryan, P. M. Lenahan, A. Y. Kang, J. F. Conley, Jr., G. Bersuker, and P. Laysaght, "Identification of the atomic scale defects involved in radiation damage in HfO_2 based MOS devices," *IEEE Trans. Nucl. Sci.*, vol. 52, no. 6, pp. 2272–2275, Dec. 2005.